

We thank two referees for their careful considerations of the manuscript and their well thoughtful comments. These certainly helped to significantly improve the paper. We've addressed all comments and questions raised, and our point-by-point responses are shown below. The referees' comments are in *Italic* and our responses are in normal font.

5 The revised manuscript is followed the response.

## Referee 1:

*This paper by Chang et al. presented a detailed analysis of five-year (2010-2015) online measurements of carbonaceous aerosols (CA) at an urban supersite in Shanghai, China.*

10 *Temporal variations of organic carbon (OC) and elemental carbon (EC) concentrations are thoroughly explored. Then, they discussed the properties of OC and EC as a function of the meteorological conditions and the air mass origin. Moreover, the authors integrated the results with historical filter-based CA measurements and satellite-based AOD observations, concluding that ambient CA concentration in*  
15 *Shanghai has decreased since 2006 after the introduction of cleaner natural gas and the control of vehicular emissions. The large data set presented in the MS are unique and important in terms of aiding the validation of atmospheric chemistry modeling and informing the effectiveness of air cleaning action to the public and policy-makers. Overall, this paper is well written and clearly describes the analysis, which addresses*  
20 *relevant scientific questions within the scope of ACP. I recommend this manuscript to be published after the following specific comments are addressed.*

Thanks for the favorable comments and the recognition of our work.

(1) *Title: the authors suggest that they are going to estimate secondary organic aerosol*  
25 *in their upcoming work. Given that the data used in their two MS are essentially the same, I suggest that the title of the current MS can be revised as "Assessment of*

*carbonaceous aerosols in Shanghai, China. Part 1: Long-term evolution, seasonal variations and meteorological effects”.*

We agree and has been revised in the MS.

- 5 (2) Page 7, lines 3-7: “concentrations of black carbon were continuously measured using an Aethalometer AE-31: 880 nm wavelength is considered as the standard channel to determine BC concentrations”. What is the mass absorption coefficient used for converting absorption coefficient to mass concentrations?

The manufacturer’s recommended value for  $\alpha_{ap}$  is  $14625/\lambda$ , which is based upon  
10 calibrations during instrument development and theoretical calculations. It has a value of  $16.6 \text{ m}^2 \text{ g}^{-1}$  at  $\lambda=880 \text{ nm}$ . This accounts for absorption by BC and additional light attenuation assumed to be caused by multiple scattering within the filter media.

- (3) Page 10, line 25: I didn’t see the citation. The difference between Sunset EC and  
15 Aethalometer BC is due to different techniques: Aethalometer is solely based on the optical technique while Sunset use the thermal-optical technique. Please note the paper by Petzold, A. et al. (2013), recommendations for reporting "black carbon" measurements, *Atmos. Chem. Phys.*, 13(16), 8365-8379, doi: 10.5194/acp-13-8365-2013.

- 20 Thanks for the recommendation of this reference. We’ve added a new reference in the revised MS (Venkatachari et al., 2006).

Reference:

Venkatachari, P., Zhou, L., Hopke, P. K., Schwab, J. J., Demerjian, K. L., Weimer, S., Hogrefe, O., Felton, D., and Rattigan, O.: An intercomparison of measurement

methods for carbonaceous aerosol in the ambient air in New York City, Aerosol Sci. Technol., 40(10), 788-795, doi: 10.1080/02786820500380289, 2006.

*(4) Page 16, lines 25-26: what is the specific chemical reactions?*

5 We've followed the suggestion given by Referee 2 to delete this sentence in the revised MS.

*(5) Conclusion: new scientific findings need more emphasis in comparison with previous work.*

10 This work represents the first multi-year and near real-time measurement study of carbonaceous aerosols in PM<sub>2.5</sub> in China. We think the most important finding is that carbonaceous aerosol pollution in Shanghai has gradually reduced since 2006, which has not been reported before. Our results confirm the success of replacing coal with cleaner energy such as natural gas in Shanghai, which can be adopted in other  
15 megacities like Beijing and Guangzhou to curb PM<sub>2.5</sub> pollution.

*(5) Table 1: this is a big table of data and difficult to take in. Could it be simplified by removing some variables?*

We agree and have deleted the variables of "OC/PM<sub>2.5</sub>" and "EC/PM<sub>2.5</sub>" in the revised  
20 MS.

## Referee 2:

*This manuscript presents a statistical analysis of long-term measurements of carbonaceous aerosols in Shanghai, China. Temporal and spatial variations of OC and EC concentration were investigated according to the observation results with reasonable scientific discussions and explanations. I recommend this article to be published after these minor comments as follows are answered properly.*

Many thanks for the encouraging comments and useful suggestions. After looking through the comments, we noticed that there were lots of minor mistakes in our original MS which can be avoided before submission. We are grateful for such generous contribution of your expertise and valuable time.

*Page 1-2: Please consider rephrasing the abstract. There are too many detailed discussions and general introductions, which make it not convenient to draw the key points from the current study. Please refer your conclusions.*

We agree that the current abstract is some sort of tediously long. We've revised the abstract as below (totally 364 words):

Carbonaceous aerosols are major chemical components of fine particulate matter (PM<sub>2.5</sub>) with major impacts on air quality, climate change, and human health. Gateway to fast-rising China and home of over twenty million people, Shanghai throbs as the nation's largest mega city and the biggest industrial hub. From July 2010 to December 2014, hourly mass concentrations of ambient organic carbon (OC) and elemental carbon (EC) in the PM<sub>2.5</sub> fraction were quasi-continuously measured in Shanghai's urban center. The annual OC and EC concentrations (mean  $\pm$  1  $\sigma$ ) in 2013 ( $8.9 \pm 6.2$  and  $2.6 \pm 2.1$   $\mu\text{g m}^{-3}$ , n=5547) and 2014 ( $7.8 \pm 4.6$  and  $2.1 \pm 1.6$   $\mu\text{g m}^{-3}$ , n=6914) were higher than that of 2011 ( $6.3 \pm 4.2$  and  $2.4 \pm 1.8$   $\mu\text{g m}^{-3}$ , n=8039) and 2012 ( $5.7 \pm 3.8$  and  $2.0 \pm 1.6$   $\mu\text{g m}^{-3}$ , n=4459). We integrated the results from historical field measurements (1999-2012) and satellite

observations (2003-2013), concluding that carbonaceous aerosol pollution in Shanghai has gradually reduced since 2006. In terms of monthly variations, average OC and EC concentrations ranged from 4.0 to 15.5 and from 1.4 to 4.7  $\mu\text{g m}^{-3}$ , accounting for 13.2-24.6% and 3.9-6.6% of the seasonal  $\text{PM}_{2.5}$  mass (38.8-94.1  $\mu\text{g m}^{-3}$ ), respectively. The concentrations of EC (2.4, 2.0, 2.2, 3.0  $\mu\text{g m}^{-3}$  in spring, summer, fall, and winter, respectively) showed little seasonal variation (excepting winter) and weekend-weekday dependence, indicating EC are a relatively stable constitute of  $\text{PM}_{2.5}$  in the Shanghai urban atmosphere. In contrast to OC (7.3, 6.8, 6.7, and 8.1  $\mu\text{g m}^{-3}$  in spring, summer, fall, and winter, respectively), EC showed marked diurnal cycles and correlated strongly with CO across all seasons, confirming vehicular emissions as the dominant source of EC at the targeted site. Our data also reveal that both OC and EC showed concentration gradients as a function of wind direction and wind speed, generally with higher values associated with winds from the southwest, west, and northwest. This was consistent with their higher potential as source areas, as determined by the potential source contribution function analysis. A common high potential source area, located along the middle and lower reaches of the Yangtze River instead of Northern China, was pinpointed during all seasons. These results demonstrate that the measured carbonaceous aerosols were driven by the interplay of local emissions and regional transport.

20

*Page 3, line 1-13: Please give proper references.*

Three relevant references have been inserted in the revised MS.

Turpin, B. J., and Huntzicker, J. J.: Secondary formation of organic aerosol in the Los Angeles basin: A descriptive analysis of organic and elemental carbon concentrations, *Atmos. Environ.*, 25, 207-215, doi: 10.1016/0960-1686(91)90291-E, 1991.

25

Bond, T. C., Doherty, S. J., Fahey, D., Forster, P., Berntsen, T., DeAngelo, B., Flanner, M., Ghan, S., Kärcher, B., and Koch, D.: Bounding the role of black carbon in the climate system: A scientific assessment, *J. Geophys. Res.*, 118, 5380-5552, doi: 10.1002/jgrd.50171, 2013.

- 5 Hallquist, M., Wenger, J. C., Baltensperger, U., Rudich, Y., Simpson, D., Claeys, M., Dommen, J., Donahue, N. M., George, C., Goldstein, A. H., Hamilton, J. F., Herrmann, H., Hoffmann, T., Iinuma, Y., Jang, M., Jenkin, M. E., Jimenez, J. L., Kiendler-Scharr, A., Maenhaut, W., McFiggans, G., Mentel, T. F., Monod, A., Prévôt, A. S. H., Seinfeld, J. H., Surratt, J. D., Szmigielski, R., and Wildt, J.: The  
10 formation, properties and impact of secondary organic aerosol: current and emerging issues, *Atmos. Chem. Phys.*, 9, 5155-5236, doi: 10.5194/acp-9-5155-2009, 2009.

*Page 3, line 28, Page 4, line 1-2, Page 4, line 3-15: What is the scientific information*

- 15 *behind this? Please consider the scientific significance or overview relating to carbonaceous aerosols, no matter the study in China or abroad.*

We are sorry for making the reviewer confused and this sentence has been deleted in the revised MS.

- 20 *Page 5, line 1-7: Was there short-term analysis of OC/EC measurements obtained from the semi-continuous OC/EC analyzer? What were their findings or the general comparison with your study?*

We appreciate the constructive comment. There are several papers (e.g., Cheng et al., *Environ. Sci. Technol.* 2015, 49, 831-838) regarding the short-term analysis of OC/EC  
25 measurements obtained from the semi-continuous OC/EC analyser in China. However,

in previous work, OC and EC were typically discussed with other PM<sub>2.5</sub> chemical components together, and it was difficult to tease out the characteristics of OC and EC. Moreover, previous work focused on the short-term (e.g., several hours to several days) formation mechanism of haze pollution, thus it makes little sense to perform a comparison with our results. The current MS is mainly about the investigation of temporal evolution of OC and EC mass concentrations. As another reviewer mentioned, there will be a companion work regarding the formation of secondary organic aerosols, in which our findings will have more opportunities to compare with previous work.

10 *Page 5, line 14: When and where, please specify.*

We've specified the sampling period (from 10 June 2010 to 31 December 2014) and location (Shanghai) in the revised MS.

*Page 5, line 24-25: Are these emission data for Shanghai or YRD, please specify.*

15 Specified as Shanghai.

*Page 5, line 27: 'urban road network' or 'urban traffic network'?*

Revised as "urban traffic network"

20 *Page 6, line 8: Please add proper references.*

Two references were added.

Turpin, B. J., Saxena, P., Andrews, E., 2000. Measuring and simulating particulate organics in the atmosphere: problems and prospects. *Atmos. Environ.* 34, 2983-3013, 2000.

NIOSH: Elemental Carbon (Diesel Particulate): Method 5040, in: NIOSH Manual of Analytical Methods, 4<sup>th</sup> edition, edited by: Eller, P. M. and Cassinelli, M. E., National Institute for Occupational Safety and Health, DHHS (NIOSH), Cincinnati, OH, USA, Publication No. 96-135, 1996.

*Page 6, line 15: There are actually four OC contents according to four different heating temperatures; have you ever analyzed them separately?*

Although the separation and discussion of OC contents is beyond the scope of this work, we think this is a useful comment and will certainly be taken into account in our future sampling work. Given the highly complex nature of OC, we are going to deploy an aerosol time-of-flight mass spectrometer to provide real-time information of OC contents.

*Page 7, line 7: Please add proper references.*

We've added a reference in the revised MS:

Arnott, W. P., Hamasha, K., W. Moosmüller, H., Sheridan, P. J., and Ogren, J. A., Towards aerosol light-absorption measurements with a 7-wavelength Aethalometer: Evaluation with a photoacoustic instrument and 3-wavelength Nephelometer, *Aerosol Sci. Technol.*, 39, 17-29, doi: 10.1080/027868290901972, 2005.



*Page 7, line 8-10: Please give specific names of all instruments, which measured CO, NO<sub>2</sub> and SO<sub>2</sub> concentration.*

According to the information provided by Shanghai Pudong Environmental Monitoring Center, ambient CO, NO<sub>2</sub> and SO<sub>2</sub> concentrations were measured by Thermo 48i, 42i,  
5 and 43i, respectively. We've added them in the revised MS.

*Page 8, line 8: Please consider rephrasing the sentence.*

We've revised the sentence as "Back trajectories analysis is a commonly used technique in atmospheric sciences, while at the city scale, back trajectories make little sense"  
10 because it was generally based on wild guess and illogical reasoning.

*Page 8, line 9-10: Please give brief explanations why BPP and PSCF are better than back trajectory analysis in your case.*

The wind speed (WS) and wind direction (WD) in BPP are measured at near ground  
15 level (18 m a.g.l), while the WS and WD in PSCF are calculated at a much higher height (typically 500 m a.g.l). Therefore, BPP is more suitable for tracing the origins of air masses at city scale.

*Page 10, line 5-6: Please rephrase the sentence.*

20 This sentence has been revised as "Between 10 June 2010 and 31 December 2014, the Sunset carbon analyser was successfully operated during 75% of the time".

*Page 10, line 14-16: Please give references.*

There are various technical definitions of four seasons, but local usage of the term varies according to local climate, cultures and customs. In most Northern Hemisphere temperate locations, spring months are March, April and May (summer is  
5 June, July, August; autumn is September, October, November; winter is December, January, February) (see <http://glossary.ametsoc.org/wiki/Spring>), although differences exist from country to country. There are several versions of “four seasons” in China. Seasons often held special significance for rural citizens in China, whose lives revolved around planting and harvest times, and the change of seasons was often attended by  
10 ritual. Nevertheless, all versions of dividing a season are very close to each other. There is no clear classification criterion to divide four seasons for investigating the characteristics of air pollutants in China. Here we adopted an unspoken or default rule to divide four seasons in Shanghai. This rule has been adopted in previous studies (e.g., Sun et al., 2015).

15 Reference:

Sun et al., Long-term real-time measurements of aerosol particle composition in Beijing, China. *Atmos. Chem. Phys.*, 15, 10149-10165, 2015

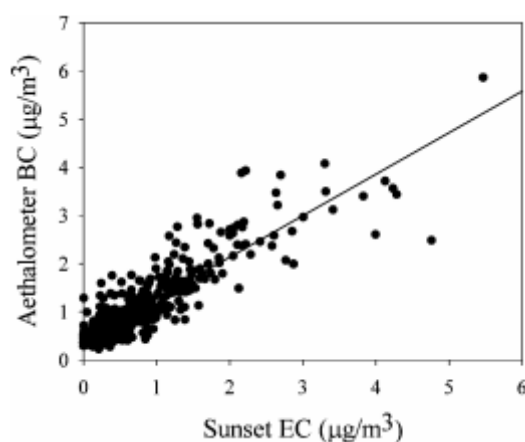
*Page 10, line 24-25: How is BC measured differently than EC? Please specify. BC is  
20 measured based on optical properties, which is light-absorptive EC, hence, it should be lower than your measured EC, please give detail explanation, for instance, did they measure light absorbance using different wavelength laser? And which earlier studies are consistent with your results? Please list them.*

Thanks for this thought-provoking comment. EC is operationally defined by their  
25 analysis method or protocol (e.g., IMPROVE/TOR, NIOSH/TOT). When the components of the ambient carbonaceous aerosol are considered thermally different,

the EC fraction is called thermal EC, and is usually determined by TOT or TOR analysis. When carbonaceous aerosol components are considered optically different, the strongly light absorbing fraction is known as BC. BC can be measured using a variety of optical absorption methods, and the Aethalometer is one of the most commonly utilized, and easy-to-use techniques employed to measure real-time BC concentrations. BC is generally produced during incomplete high-temperature combustion. It is affected to a limited extent by atmospheric processing and is therefore a direct tracer for combustion emissions. The various chemical and physical properties of the EC may cause changes in the measured optical BC concentrations even if the same measurement system is used.

The measurement of BC is complicated by the lack of a simple definition of BC and the absence of techniques that are uniquely sensitive to BC. We agree with the reviewer that BC is essentially light-absorptive EC. Practically, despite multiple wavelengths operated, the Aethalometer generally treats light-absorptive carbon as BC (equivalent black carbon), which may overestimate BC concentration because the presence of light-absorptive organic carbon, also known as brown carbon. The BC measurements used here are based on the 880-nm wavelength to minimize potential interference from brown carbon.

Although EC concentration is generally higher than BC concentration, our results are generally consistent with Venkatachari et al (2006).



Reference:

Venkatachari P, Zhou L, Hopke P K, et al. An intercomparison of measurement methods for carbonaceous aerosol in the ambient air in New York City. *Aerosol Science and Technology*, 2006, 40(10): 788-795.

5 *Page 11, line 1-2: what kind of different thermal, optical and chemical behavior during springtime as you expect?*

Eastern China (including Shanghai) has a monsoon subtropical climate, which means that different seasons may have different regional-transported sources of EC. The changes in OC to EC ratios also exhibit seasonal patterns. Spring is the time when many  
10 plants begin to grow and flower, leading to a higher OC/EC ratio as indicated in previous work. Also, the late of May in Eastern China is one of the most important period of biomass burning (burning of crop residues). Although we failed to provide qualitative evidence, biomass burning-emitted EC may have very different thermal, optical and chemical behaviours from vehicle-emitted EC. The various chemical and  
15 physical properties of the EC may cause changes in the measured optical BC concentrations even if the same measurement system is used (Jeong et al. 2004).

Reference:

Jeong, C. H., Hopke, P. K., Kim, E., and Lee, D. W. (2004). The Comparison Between Thermal-Optical Transmittance Elemental Carbon and Aethalometer Black Carbon  
20 Measured at Multiple Monitoring Sites, *Atmos. Environ.* 38:5193–5204.

*Page 11, line 9: Your PM<sub>2.5</sub> measurement was only started from 2013, so please reword your sentence.*

The sentence has been revised as “..., contributing on average ~20% (OC) and ~5.0%  
25 (EC) to the PM<sub>2.5</sub> mass between 2013 and 2014”.

*Page 11, line 10-12: This is a scientific article; it is better not only report data. Please give short or brief discussion, even though you give extensive discussions elsewhere.*

Agree, and in the revised MS, we've compared our results with previous study  
5 performed in the Yangtze River Delta region (e.g., 2.4 in Nanjing City (Chen et al., 2017)). A much higher OC/EC ratio in our study (3.7) indicates that secondary organic aerosol is more important in Shanghai.

Reference:

Chen, D., Cui, H., Zhao, Y., Yin, L., Lu, Y., and Wang, Q.: A two-year study of  
10 carbonaceous aerosols in ambient PM<sub>2.5</sub> at a regional background site for western Yangtze River Delta, China, Atmos. Res., 183, 351-361, doi: 10.1016/j.atmosres.2016.09.004, 2017a.

*Page 11, line 15: 56% and 23% of what?*

15 We've clarified in the revised MS as "56% and 23% of observed PM<sub>2.5</sub> mass concentrations".

*Page 11, line 17-19: Please consider rewording your sentence.*

The original sentence has been revised as "Carbonaceous aerosols contribute a small  
20 fraction (22%) of PM<sub>2.5</sub> when PM<sub>2.5</sub> mass concentration greater than 140  $\mu\text{g m}^{-3}$ . However, carbonaceous aerosols dominate the chemical components of PM<sub>2.5</sub> ( $\approx 50\%$ ) when PM<sub>2.5</sub> concentration lower than 30  $\mu\text{g m}^{-3}$ ".

*Page 11, line 20: Should primary inorganic aerosol also contribute?*

Yes, we've deleted "secondary" in the revised MS. Shanghai has a subtropical monsoon climate and is bounded to the east by the East China Sea, and the SE winds originating from the East China sea prevail in summers and fall. Therefore, the urban atmosphere  
5 of Shanghai is likely to be a receptor of primary inorganic aerosol like sea salts.

*Page 11-12, line 25-end: In a scientific article, it is better not give such massive information and description of the local policies. And I doubt you can conclude that these policies have been ineffective in this study according to your simple observation  
10 data.*

Agree and we've deleted this sentence in the revised MS.

*Page 12, line 8: What does your OC frequency mean in Fig. 4? Please specify in your method part.*

15 We've added in the revised MS. The frequency was calculated based on the average data points within a mass concentration interval of  $0.5 \mu\text{g m}^{-3}$  and  $2 \mu\text{g m}^{-3}$  for EC and OC, respectively.

*Page 12, line 11: Please add references for the discussions on the most severely  
20 polluted month*

Two relevant references have been cited in the revised MS:

Huang, R. J., Zhang, Y., Bozzetti, C., Ho, K. F., Cao, J. J., Han, Y., Daellenbach, K. R.,  
Slowik, J. G., Platt, S. M., Canonaco, F., Zotter, P., Wolf, R., Pieber, S. M., Bruns,

E. A., Crippa, M., Ciarelli, G., Piazzalunga, A., Schwikowski, M., Abbaszade, G., Schnelle-Kreis, J., Zimmermann, R., An, Z., Szidat, S., Baltensperger, U., El Haddad, I., and Prevot, A. S.: High secondary aerosol contribution to particulate pollution during haze events in China, *Nature*, 514, 218-222, 10.1038/nature13774, 2014.

- 5 Zhang, Y. L., Huang, R. J., El Haddad, I., Ho, K. F., Cao, J. J., Han, Y., Zotter, P., Bozzetti, C., Daellenbach, K. R., Canonaco, F., Slowik, J. G., Salazar, G., Schwikowski, M., Schnelle-Kreis, J., Abbaszade, G., Zimmermann, R., Baltensperger, U., Prévôt, A. S. H., and Szidat, S.: Fossil vs. non-fossil sources of fine carbonaceous aerosols in four Chinese cities during the extreme winter haze episode of 2013, *Atmos. Chem. Phys.*, 15, 1299-1312, doi: 10.5194/acp-15-1299-2015, 2015a.

*Page 12, line 11-13: I don't understand your statement here, please reword your sentence and give appropriate explanation.*

- 15 Please refer to our response to the next comment (*Page 12, line 19*).

*Page 12, line 19: You concluded previously that the pollution control policies are ineffective; however, here you said the air-cleaning measures are successful. Please be consistent.*

- 20 As we stated in the MS, China (including Shanghai) experienced extremely severe and persistent haze pollution in the first quarter of 2013, thus it “**seems**” that previous pollution control policies are ineffective. However, a higher carbonaceous aerosol loading in 2013 may be an exception due to the influence of unfavorable meteorology. There is a need to put our study into a longer time frame so that we can obtain a panoramic view of the inter-annual evolution of carbonaceous aerosols levels in Shanghai. After integrating satellite-based observation of AOD (2000-2013) and

ground-based measurements of OC-EC and SO<sub>2</sub> (2003-2015), we finally conclude that air-cleaning measures in Shanghai are successful.

*Page 12, line 23-25: Please give proper references here.*

5 Two relevant references have been cited in the revised MS:

Schauer, J. J., Mader, B. T., Deminter, J. T., Heidemann, G., Bae, M., Seinfeld, J., Flagan, R., Cary, R., Simith, D., Huebert, B., Bertram, T., Howell, S., Kline, J., Quinn, P., Bates, T., Turpin, B., Lim, H., Yu, J., Yang, H., and Keywood, M.: ACE-Asia intercomparison of a thermal-optical method for the determination of particle-phase organic and elemental carbon, Environ. Sci. Technol., 37(5): 993-1001, doi: 10.1021/es020622f, 2003.

Karanasiou, A., Minguillón, M. C., Viana, M., Alastuey, A., Putaud, J.-P., Maenhaut, W., Panteliadis, P., Močnik, G., Favez, O., and Kuhlbusch, T. A. J.: Thermal-optical analysis for the measurement of elemental carbon (EC) and organic carbon (OC) in ambient air a literature review, Atmos. Meas. Tech. Discuss., 8, 9649-9712, doi: 10.5194/amtd-8-9649-2015, 2015.

*Page 12, line 29: How was it validated by the evolution of SO<sub>2</sub> concentration, please specify.*

20 We've specify it in the revised MS. Over 90% of SO<sub>2</sub> emissions in China were derived from coal combustion (Lu et al., 2011), and ambient SO<sub>2</sub> concentrations were directly related to SO<sub>2</sub> emissions. Therefore, the long-term evolution of SO<sub>2</sub> concentration, to a large extent, reflects the evolution of coal consumption in China.

Reference:



Lu, Z., Zhang, Q., and Streets, D. G.: Sulfur dioxide and primary carbonaceous aerosol emissions in China and India, 1996-2010, *Atmos. Chem. Phys.*, 11, 9839-9864, <https://doi.org/10.5194/acp-11-9839-2011>, 2011.

5 *Page 13, line 12: It is really difficult to read Fig. 6, especially each subplot. Please consider replot them. For monthly and seasonal variations, I would suggest a figure plotting the average or medium concentrations of each month or each season during all these years. Then give further discussions regarding to the new figure.*

We guess that the difficulty for the reviewer to read Fig. 6, to a large extent, is because  
10 of the low resolution of figure in the current form. In fact, the Fig. 6 was plotted exactly followed the reviewer's suggestion. For example, Fig. 6b shows the monthly variations of EC and OC. We first plotted the monthly average (indicated by filled circles) values of EC and OC and their standard variations (indicated by vertical lines) in different year (please zoom in on the X axis to see more detail), then we plotted the monthly  
15 concentrations of EC and OC during all these 5 years (please see the two relatively smaller figures in Fig. 6b).

We've uploaded our original high-resolution figures, and hopefully it is easy to follow for the readers.

20 *Page 13, line 26-27: I would like to see the comparison of the concentration of OC from different seasons but of the same year.*

As shown in Table 1, different year show different seasonal variations of OC concentration. For example, in 2010, OC conc. shown the highest in winter, followed by fall, summer. However, in 2011, OC conc. in spring > winter > summer > fall. This  
25 can be explained by the complexity of OC in terms of the formation processes and sources (see detailed discussion in section 3.2.4 and 3.3).

*Page 14, line 19-22: I don't get it. Please reword it.*

We've reworded this sentence as "The highest degree of correlation ( $R^2 = 0.71$ ) was observed during wintertime when the seasonal OC/EC ratio was the lowest (Table 1),  
5 suggesting that primary emissions are an important source contributing to both OC and EC in Shanghai during the cold season".

*Page 14, line 25, or Page 35, 37: Please make your figure caption more clearly. Which one is for weekdays and which one is for weekend?*

10 We've added the specific row and column in the text to make our description clear, e.g., "fall of 2012 (the third row, the second column)".

*Page 14 line 25 to Page 15, line 9: I suggest you plot the mass fraction of EC and OC in  $PM_{2.5}$  or  $PM_{10}$  first and then give the conclusions.*

15 We didn't have  $PM_{10}$  data in the current study. Since October 2016, an 8-stages PM sampler was deployed at the Shanghai Pudong supersite. We look forward to showing the size-segregated EC and OC aerosols in the near future.

20 *Page 15, line 17 to 24: This paragraph has nothing to do with the explanation of the diurnal patterns of EC and your CO emissions. Or at least it is not written in a clear way to explain your scientific issues here, please consider rewrite it.*

Agree, and we've deleted this paragraph in the revised MS.

*Page 15, line 25: The scatter plots of EC vs. CO in Fig. 9 cannot confirm that on-road traffic is an important source contributing to EC emissions in Shanghai. You need to cite similar works from others to support your conclusions here.*

Agree, and we've cited two similar works in China to support our conclusion.

- 5 1. Chen, D., Cui, H., Zhao, Y., Yin, L., Lu, Y., and Wang, Q.: A two-year study of carbonaceous aerosols in ambient PM<sub>2.5</sub> at a regional background site for western Yangtze River Delta, China, *Atmos. Res.*, 183, 351-361, doi: 10.1016/j.atmosres.2016.09.004, 2017.
2. Yang, F., He, K., Ye, B., Chen, X., Cha, L., Cadle, S. H., Chan, T., and Mulawa, P.  
10 A.: One-year record of organic and elemental carbon in fine particles in downtown Beijing and Shanghai, *Atmos. Chem. Phys.*, 5, 1449-1457, <https://doi.org/10.5194/acp-5-1449-2005>, 2005.

Still, CO variation can be utilized as a robust indicator of vehicle emissions in Shanghai. Historically, CO emissions in Shanghai and its surrounding YRD region mainly came  
15 from iron and steel manufacturing and on-road vehicles, which contributed 34% and 30% of the total, respectively in 2007 (Huang et al., 2011). Due to changing economic activity, emission sources of air pollutants in China are changing rapidly. For example, over the past several years, China has implemented a portfolio of plans to phase out its old-fashioned and small steel mills, and raise standards for industrial pollutant  
20 emissions (Chang et al., 2012). In contrast, China continuously experienced double digit growth in terms of auto sales during the same period, and became the world's largest automobile market since 2009 (Chang, 2014). Consequently, on-road traffic has overtaken industrial sources as the dominant source of CO emissions in Eastern China (Zhao et al., 2012). In our previous work in Shanghai (Chang et al., 2016), CO shows  
25 a well-marked bimodal diurnal profile, with maxima in the morning (starting at 05:00

local time) and the evening (starting at 16:00), consistent with the variation of traffic flow in Shanghai (Liu et al., 2012).

Reference:

- Huang, C., Chen, C. H., Li, L., Cheng, Z., Wang, H. L., Huang, H. Y., Streets, D., Wang, Y., Zhang, G., and Chen, Y. R.: Emission inventory of anthropogenic air pollutants and VOC species in the Yangtze River Delta region, China, *Atmos. Chem. Phys.*, 11(9), 4105-4120, doi: 10.5194/acp-11-4105-2011, 2011.
- Chang, Y. H.: Non-agricultural ammonia emissions in urban China, *Atmos. Chem. Phys. Discuss.*, 14(6), 8495-8531, doi: 10.5194/acpd-14-8495-2014, 2014.
- 10 Chang, Y. H., Liu, X., Dore, A. J., and Li, K.: Stemming PM<sub>2.5</sub> pollution in China: Re-evaluating the role of ammonia, aviation and non-exhaust road traffic emissions, *Environ. Sci. Technol.*, 46(24), 13035-13036, doi: 10.1021/es304806k, 2012.
- Chang, Y., Zou, Z., Deng, C., Huang, K., Collett, J. L., Lin, J., and Zhuang, G.: The importance of vehicle emissions as a source of atmospheric ammonia in the megacity of Shanghai, *Atmos. Chem. Phys.*, 16, 3577-3594, <https://doi.org/10.5194/acp-16-3577-2016>, 2016.
- 15 Liu, Y., Wang, F. Xiao, Y., and Gao, S: Urban land uses and traffic ‘source-sink areas’: Evidence from GPS-enabled taxi data in Shanghai, *Landscape Urban Plan.*, 106(1), 73-87, doi: 10.1016/j.landurbplan.2012.02.012, 2012.
- 20 Zhao, Y., Nielsen, C. P., McElroy, M. B., Zhang, L., and Zhang, J.: CO emissions in China: Uncertainties and implications of improved energy efficiency and emission control, *Atmos. Environ.*, 49, 103-113, doi: 10.1016/j.atmosenv.2011.12.015, 2012.

*Page 15, line 27: Where does it show the multi-day build-up of OC for all months in*

*your Fig. 3. Sorry I cannot capture it. Please specify.*

The Fig. 3 should be corrected as Fig. 4, and we've corrected in the revised MS.

*Page 15, line 28: I have huge difficulties to read your figures in your manuscript, as*

5 *the order of your figures are completely messed up. Please consider reorder all your figures in your manuscript.*

Deeply sorry for making such rookie mistake! We've corrected the mess of the order of figures in the revised MS.

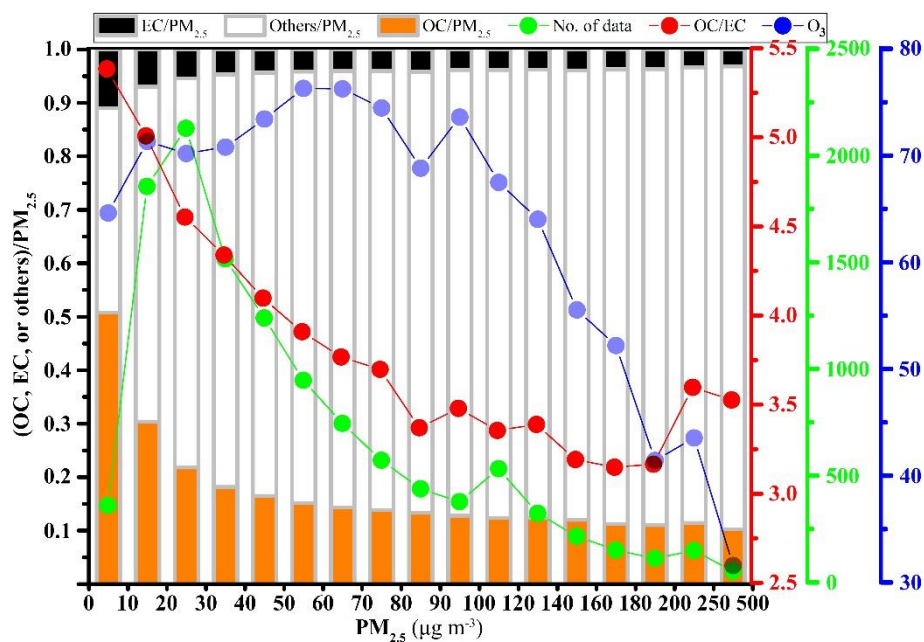
10 *Page 16, line 5: The increase as you stated could only be observed for the data during fall of 2010 and 2012. As I seen, your diurnal patterns of the OC con vary by seasons and also by years. The complexity of the diurnal variation of OC, however, suggests the OC you measured were from different sources, both primary and secondary. It is really difficult to estimate only one OC emission source from your current data.*

15 We confess that estimated solely based on our current data, it is difficult to pinpoint a specific OC emission source. Therefore, we've added the potential limitation and soften our claim in the revised MS as "In this study, OC in fall and winter showed a clear daytime increase until late afternoon, illustrating possible role played by gas-phase photochemical processing in driving the OC diurnal cycle. However, it should be  
20 noticed that it is still difficult to pinpoint a specific OC emission source based on our current data. Since ambient OC concentration depends on multiple factors, further study will reveal more information about the different formation mechanisms involved".

Page 16, line 14: This is actually quite interesting result from Fig. 11a. (Here, again, how could you talk about Fig. 11b first, then Fig. 11a? It is difficult to follow.) There is obvious correlation, but not linear relationship. It will be more interesting if you could find out the changes of PM loadings or other trace gaseous concentration at  $O_3 > 60$  and  $O_3 < 60$ , which might support what stated in the following part at current section.

We've corrected the mess of the order of figures in the revised MS. Again, sorry for making the difficulty to follow.

We admire the reviewer for his/her shrewder observation. Indeed, setting  $O_3 = 60$  as a breaking point, the linear correlation between  $O_3$  and OC can be shifted from negative ( $O_3 < 60$ ) to positive ( $O_3 > 60$ ) as indicated in the figure below. In fact, this interesting result has been involved in our upcoming work regarding the formation of secondary organic aerosols in Shanghai.



Page 16, line 25: I don't fully agree with you. Higher  $T$  does not necessarily mean stronger solar radiation intensity. It also depends on your cloudiness. And at higher  $T$ , normally your OC evaporates more, which could not explain what you observed here.

We agree, and we've deleted this sentence in the revised MS.

*Page 17, line 1-5: Similarly, at low T, the evaporation of OC is slow that it is reasonable to observe a higher OC concentration at low T. However, OC/EC is less than 2, which means the emissions of EC was quite high at those conditions, which you discussed in the next section. Please always combine OC and EC together when you discuss OC/EC ratio.*

Thanks for the suggestion, and we've combined the discussion of OC/EC ratio with OC or EC in the revised MS. The current work is mainly focus on the discussion in terms of the mass concentrations and temporal variations of EC and OC, and a detailed discussion regarding secondary organic aerosols (including OC/EC ratio) will be presented in our next work.

*Page 17, line 6-11: Could that be your primary emissions of EC is high at low T, or winter time, as suggested by your Fig. 9. Please refer the absolute value of EC and CO. And why the WS-dependence of EC concentration is not valid for OC?*

On-road traffic and biomass burning (especially burning of crop residues) are two major sources of EC emissions in China, and biomass burning activities are concentrated in summer and generally rare during wintertime. As to traffic-emitted EC, there is no evidence to show a clear relationship between ambient temperature and emission amount. In Fig. 9, the absolute values of both EC and CO are much higher than other seasons, and this is not necessarily the result of higher emissions in winter but more likely due to a lower PBHL (Chang et al., 2016) and stronger regional transport during wintertime (discussed in latter section).

A greater dependence on wind speed for EC than OC is because that EC is primarily originated from local traffic emissions while OC is the complex product of primary emission (mainly local sources) and secondary formation (long-range transport and atmospheric ageing).

5    Reference:

Chang, Y., Zou, Z., Deng, C., Huang, K., Collett, J. L., Lin, J., and Zhuang, G.: The importance of vehicle emissions as a source of atmospheric ammonia in the megacity of Shanghai, Atmos. Chem. Phys., 16, 3577-3594, <https://doi.org/10.5194/acp-16-3577-2016>, 2016.

10

*Page 17, line 13-20: Please add the correlation coefficient of OC or EC vs. WS.*

In Figure 13, the data of OC, EC, and WS were divided as several groups and presented as box-and-whisker plot instead of scatter plot with individual data points; therefore, the correlation coefficients of OC or EC vs. WS are not calculated in this study.

15

*Page 18, line 5-6: What is your expected reason?*

The primary reason is because of the different source regions between carbonaceous aerosols (Southwest Shanghai) and coal-related pollutants like sulfate (Northern China), which had been further discussed in the latter section.

20

*Page 18, line 15: Which urban districts of Shanghai? Should the air mass from SW be your major source for EC?*

Sorry for making this confusion. Yes, the urban districts of Shanghai are in its SW. We've revised as "Given the relatively low WS ( $< 6 \text{ m s}^{-1}$  in most cases; Fig. 14) in the



SW (where the main urban districts located), the urban areas of Shanghai were highly likely the major source areas for EC”.

*Page 18, line 19: I am not sure this is fully correct. It is more depending on your back*

5 *trajectory of the air mass, but not winds from Siberia, as it is quite clean background.*

Shanghai has a humid subtropical climate and experiences four distinct seasons. Winters are chilly and damp, with northwesterly winds from Siberia can cause nighttime temperatures to drop below freezing, although most years there are only one or two days of snowfall. Despite the clean air in Siberia, winter air masses from Siberia  
10 will mixed with extremely polluted air in Northern China (Huang et al., 2014).

We’ve revised as “with northwesterly winds from Siberia transporting high levels of air pollutants in Northern China to the YRD region resulting in poor air quality in Shanghai” in the revised MS to avoid potential misunderstanding.

Reference:

15 Huang R J, Zhang Y, Bozzetti C, et al. High secondary aerosol contribution to particulate pollution during haze events in China. *Nature*, 2014, 514(7521): 218-222. doi:10.1038/nature13774.

*Page 18, line 24 to Page 19: What does rice-growing areas and biomass burning  
20 activity have any relationship with your PSCF or your current section (meteorological effect)? In which area, does the biomass burning occur normally in China, which contributes the EC concentration in Shanghai?*

In this study, we found that the transport pathways of air masses (indicated by PSCF analysis) were highly overlapped with China’s major rice-growing areas, and the PSCF

analysis was essentially related to the meteorological parameters like wind speed and wind direction. Biomass burning activities in China do not occur as normal as tropical countries and areas, but it is still an important source of air pollutants (e.g., organic aerosols) in China (Zou et al., 2017). In Eastern China, there are two typical periods of intensive biomass burning, i.e., the end of May and the beginning of November, largely due to the burning of crop residues in the North China Plain (wheat) and along the lower reaches of the Yangtze River (rice). The lower reaches of the Yangtze River had been identified as the major source region contributing to EC concentration in Shanghai previously (Cheng et al., 2014).

10    Reference:

Zhou, Y., Xing, X., Lang, J., Chen, D., Cheng, S., Wei, L., Wei, X., and Liu, C.: A comprehensive biomass burning emission inventory with high spatial and temporal resolution in China, *Atmos. Chem. Phys.*, 17, 2839-2864, doi:10.5194/acp-17-2839-2017, 2017.

- 15    Cheng, Z., Wang, S., Fu, X., Watson, J. G., Jiang, J., Fu, Q., Chen, C., Xu, B., Yu, J., Chow, J. C., and Hao, J.: Impact of biomass burning on haze pollution in the Yangtze River delta, China: a case study in summer 2011, *Atmos. Chem. Phys.*, 14, 4573-4585, <https://doi.org/10.5194/acp-14-4573-2014>, 2014.

20    *Page 19, line 11: What is the anthropogenic influence you stated here? Please specify.*

*Should biomass burning belong to anthropogenic activity?*

Thanks for the suggestion. We would like to clarify that we had specified the anthropogenic influence in lines 12-15, i.e., rapid urbanization process and massive industrial production. For biomass burning, pollutants' emissions from prescribed burning (e.g., forest clearing, burning of crop residues) and fireplace/woodstove

25

activities are also anthropogenic origin, while these were not included in our discussion of “anthropogenic influence”. Therefore, we’ve clarified this in revised MS.

*Page 19, line 15-line 18: Please consider removing it and giving your scientific*  
5 *understanding of the PSCF you plotted in Fig. 15.*

We’ve removed this sentence and replaced as “In brief, our PSCF analysis highlighted the importance of long-range transport contributing to OC pollution in Shanghai”.

10

15

20

# Assessment of carbonaceous aerosols in Shanghai, China,

## Part 1: Long-term evolution, seasonal variations and meteorological effects

Yunhua Chang<sup>1</sup>, Congrui Deng<sup>2</sup>, Fang Cao<sup>1</sup>, Chang Cao<sup>1</sup>, Zhong Zou<sup>3</sup>, Shoudong Liu<sup>1</sup>, Xuhui Lee<sup>1</sup>, Jun Li<sup>4</sup>, Gan Zhang<sup>4</sup>, and Yanlin Zhang<sup>1,\*</sup>

<sup>1</sup>Yale-NUIST Center on Atmospheric Environment, Nanjing University of Information Science and Technology, Nanjing 10044, China

<sup>2</sup>Shanghai Key Laboratory of Atmospheric Particle Pollution and Prevention (LAP<sup>3</sup>), Department of Environmental Science and Engineering, Fudan University, Shanghai 200433, China

<sup>3</sup>Pudong New Area Environmental Monitoring Station, Shanghai 200135, China

<sup>4</sup>State Key Laboratory of Organic Geochemistry, Guangzhou Institute of Geochemistry, Chinese Academy of Sciences, Guangzhou 510640, China

*Correspondence to:* Yanlin Zhang (dryanlinzhang@outlook.com or yanlinzhang@nuist.edu.cn)

**Abstract** Carbonaceous aerosols are major chemical components of fine particulate matter (PM<sub>2.5</sub>) with major impacts on air quality, climate change, and human health. Gateway to fast-rising China and home of over twenty million people, Shanghai throbs as the nation's largest mega city and the biggest industrial hub. From July 2010 to December 2014, hourly mass concentrations of ambient organic carbon (OC) and elemental carbon (EC) in the PM<sub>2.5</sub> fraction were quasi-continuously measured in Shanghai's urban center. The annual OC and EC concentrations (mean  $\pm$  1  $\sigma$ ) in 2013 (8.9 $\pm$ 6.2 and 2.6 $\pm$ 2.1  $\mu\text{g m}^{-3}$ , n=5547) and 2014 (7.8 $\pm$ 4.6 and 2.1 $\pm$ 1.6  $\mu\text{g m}^{-3}$ , n=6914) were higher than that of 2011 (6.3 $\pm$ 4.2 and 2.4 $\pm$ 1.8  $\mu\text{g m}^{-3}$ , n=8039) and 2012 (5.7 $\pm$ 3.8 and 2.0 $\pm$ 1.6  $\mu\text{g m}^{-3}$ , n=4459). We integrated the results from historical field measurements (1999-2012) and satellite observations (2003-2013), concluding that carbonaceous aerosol pollution in Shanghai has gradually reduced since 2006. In terms of monthly variations, average OC and EC concentrations ranged from 4.0 to 15.5 and from 1.4 to 4.7  $\mu\text{g m}^{-3}$ , accounting for 13.2-24.6% and 3.9-6.6% of the seasonal PM<sub>2.5</sub> mass (38.8-94.1  $\mu\text{g m}^{-3}$ ), respectively. The concentrations of EC (2.4, 2.0, 2.2, 3.0  $\mu\text{g m}^{-3}$  in spring, summer, fall, and winter, respectively) showed little seasonal variation (excepting winter) and weekend-weekday dependence, indicating EC are a relatively stable constituent of PM<sub>2.5</sub> in the Shanghai urban atmosphere. In contrast to OC (7.3, 6.8, 6.7, and 8.1  $\mu\text{g m}^{-3}$  in spring, summer, fall, and winter, respectively), EC showed marked diurnal cycles and correlated strongly with CO across all seasons, confirming vehicular emissions as the dominant source of EC at the targeted site. Our data

also reveal that both OC and EC showed concentration gradients as a function of wind direction and wind speed, generally with higher values associated with winds from the southwest, west, and northwest. This was consistent with their higher potential as source areas, as determined by the potential source contribution function analysis. A common high potential source area, located along the middle and lower reaches of the Yangtze River instead of Northern China, was pinpointed during all seasons. These results demonstrate that the measured carbonaceous aerosols were driven by the interplay of local emissions and regional transport.

## 1 Introduction

Atmospheric carbonaceous aerosols comprise 10-70% of PM<sub>2.5</sub> (atmospheric particulate matter with aerodynamic diameters equal or less than 2.5 µm) mass with particularly high levels found in urban atmospheres (Turpin et al., 2000)[E:\1 " ENREF 25" \o "Pöschl, 2005 - 3670" .](#) Broadly, carbonaceous aerosols have three categories, namely organic carbon (OC), elemental carbon (EC; loosely also known as black carbon (BC), and carbonate carbon (CC) (Turpin et al., 2000; Bond et al., 2013). OC is carbon associated with organic compounds either directly emitted to the atmosphere (primary OC, POC) or formed by the condensation of compounds produced via the atmospheric photochemical reaction of anthropogenic and biogenic volatile organic precursors (secondary OC, SOC) (Turpin and Huntzicker, 1991; Hallquist et al., 2009). EC is exclusively of primary origin and essentially nonvolatile, formed from incomplete combustion of fossil fuel such as automobile engines (especially diesel vehicles), coal, or biomass burning through thermal degradation of organic materials. CC, typically present in natural mineral dust and building/demolition dust, exists mainly in the coarse fraction and was found to be negligible in some studies (Sillanpää, 2005; Chow and Watson, 2002).

Gathering evidence has shown a consistent association of the mass concentrations of carbonaceous aerosols with a range of local to global challenges including air pollution (Castro et al., 1999; Cao et al., 2007; Huang et al., 2014), visibility impairment (Park et al., 2003; Cao et al., 2012; Volkamer et al., 2006), health damage (Pope III et al., 2002; Samet et al., 2000; Qiao et al., 2014; Lim et al., 2012), and climate change (Bond et al., 2013; Gustafsson et al., 2009; Jacobson, 2001). China is thought to be one of the leading contributors to the global burden of carbonaceous aerosols emissions (Cao et al., 2006; Klimont et al., 2009; Fu et al., 2012; Li et al., 2009; Cui et al., 2015), and this can be largely explained

by its fast urbanization rate coupled with rapid industrial development in its economically developed regions (Fang et al., 2016; Zhao et al., 2015; Lin et al., 2014), such as Beijing-Tianjin-Hebei (BTH), the Yangtze River Delta (YRD; cities such as Shanghai, Nanjing and Hangzhou), and the Pearl River Delta (PRD; cities like Guangzhou, Shenzhen and Hong Kong). Estimated from the “bottom-up” methodology, the nation’s vehicular emissions of BC and OC increased significantly from 47.1 Tg and 74.4 Tg in 1999 to 177.6 Tg and 101.5 Tg in 2011 (Cui et al., 2015). Co-emitted with EC and POC from on-road traffic, NMVOC (Non-methane Volatile Organic Compounds) emissions can also be expected to experience a similar trajectory (Li et al., 2015). Nevertheless, it is worth noting that vehicle-related emissions in China lagged significantly behind its double-digit growth in annual automobile sales in the 2000s (Chang et al., 2016) due to implementation of policy to curb vehicular emissions.

Change has come to China. China’s National Ambient Air Quality Standard (NAAQS) implemented regulations to control PM<sub>10</sub>, NO<sub>x</sub> and SO<sub>2</sub> concentrations in the 1990s. Starting from 2005, China had bypassed the national goal of a 10% reduction in SO<sub>2</sub> emissions as of 2010 (achieving a 14.3% reduction), and NO<sub>x</sub> emissions also had a plan to be 10% lower than the benchmark of 2010 (Chang, 2012). The focus is now on PM<sub>2.5</sub>. In 2013, China unveiled its five-year “Ten-point air plan”, a comprehensive guideline calls for nationwide improvements in air quality by 2017, aiming to cut PM<sub>2.5</sub> levels by 25%, 20%, 15% in the regions of BTH, YRD, and PRD, respectively (MEP, 2013). Other quantified targets for 2017 include a drop of around 20% in the energy intensity of industrial added value on 2012 levels; and a fall in the percentage of coal use in total energy consumption to 65% or less. Besides, 150 billion cubic meters of new natural gas pipeline capacity will come online in the three key regions by 2015. The plan lists 33 measures to achieve the targets, including further incentives for new-energy vehicles, fuel quality improvements, dealing with small coal furnaces and reductions in coal use in the three key regions (Zhang et al., 2017).

Previous field sampling studies have shown that carbonaceous aerosols in many Chinese cities account for 20 to 50% of PM<sub>2.5</sub> mass (Cao et al., 2004; Cao et al., 2005; Cao et al., 2007; Duan et al., 2005; Zhang et al., 2008b; He et al., 2001; Cao et al., 2013; Duan et al., 2007; Zheng et al., 2005; Zhang et al., 2008a). Based on daily PM<sub>2.5</sub> filter samples and the IMPROVE protocol, Cao et al., (2007) performed the first nationwide simultaneous measurements of OC and EC in 14 cities in China during winter and summer seasons in 2003. A one-year (2006) 24-hr sampling campaign carried out at 18 different sites (including

rural, urban and remote locations) was reported in (Zhang et al., 2008b), in which they provided unique insights into the seasonal and spatial variations of carbonaceous aerosol pollution across China. More recently, radiocarbon-based source apportionment of carbonaceous aerosols has been applied in China (Zhang et al., 2014; Zhang et al., 2012; Zhang et al., 2015a; Zhang et al., 2016). Nevertheless, long-term  
5 monitoring strategies based on the analysis of aerosols sampled on filters are subject to various sampling and analytical artifacts (Arhami et al., 2006; Cheng et al., 2009; Wu et al., 2016; Turpin et al., 1994); they are labor-intensive and time consuming; moreover, they fail to capture processes governing diurnal variations of atmospheric pollutants and cannot provide precise diagnostics during pollution episodes. In this context, the Sunset Laboratory semi-continuous OC/EC analyzer is capable of providing near-real-  
10 time information of artifact-free measurement of carbonaceous aerosols, and has greatly improved the understanding of the sources and transformation processes of carbonaceous aerosols. However, due to the maintenance cost and intensive calibration requirements the semi-continuous OC/EC analyzer has rarely been used for long-term monitoring in China. Besides, auxiliary instruments related to aerosol chemical components and optical properties have not previously been applied to aid OC/EC data quality  
15 check and PM source apportionment.

In response to these deficiencies and needs, an in situ atmospheric superstation has been implemented in 2010 at Shanghai urban center, allowing the chemical, physical and optical characterization of PM pollution for the largest megacity in China. As the biggest megacity in China, Shanghai is one of several cities pioneering the implementation of new policies or adopting advanced technologies to curb air  
20 pollution since 2000s. Therefore, the evolution of air pollution in Shanghai, to a large extent, exemplifies the progresses and challenges toward cleaning China's air. In this study, we describe and discuss the longest (from 10 June 2010 to 31 December 2014) on-line field measurement of carbonaceous aerosols in Shanghai, China obtained by a Sunset online OC/EC analyzer, aiming to elucidate their variation characteristics and geographical origins, examine the effects of meteorological factors on measured  
25 carbonaceous aerosols, and assess the effectiveness of control measures taken in Shanghai. Future work will focus on the sources and formation mechanisms of carbonaceous aerosols.

## 2 Experiment

### 2.1 Site description

Covering 6340.5 km<sup>2</sup> of land area and enjoying the largest commercial and industrial hub in China (Fig. 1), Shanghai is home to a population of over 24 million people and 2.7 million vehicles (0.3 million of which are diesel engines) according to figures from 2013 (China Automotive Industry Yearbook, 2014). The emissions of SO<sub>2</sub>, NO<sub>x</sub>, PM<sub>10</sub>, PM<sub>2.5</sub>, BC, OC, NMVOC, and NH<sub>3</sub> in Shanghai in 2010 were estimated as 620.3, 468.0, 160.0, 112.0, 12.5, 10.5, 541.4, and 61.8 Mg, respectively (Huang et al., 2011). Field measurements were carried out at the Pudong Environmental Monitoring Center (PEMC; 121.5447°E, 31.2331°N), which is located in southwest urban Shanghai with an intensive urban road network (SI Fig. S1). There were no major industrial sources nearby. The sampler inlet was on the rooftop of a 5-floor building (~18 m above the ground). There were no buildings obstructing observations at this height and the air mass could flow smoothly through the local area. The detailed description of the sampling site is given elsewhere (Chang et al., 2016).

### 2.2 Field measurements

Hourly ambient OC and EC concentrations were recorded from 10 June 2010 to 31 December 2014 through a Sunset Laboratory semi-continuous OC/EC analyzer (RT-4 model, Sunset Lab. Inc., USA). The analyzer was based on the NIOSH method 5040 and employs the thermal-optical transmittance (TOT) protocol for pyrolysis correction (Turpin et al., 2000; NIOSH, 1996). Ambient air was input with a flow rate of 8 LPM through a PM<sub>2.5</sub> sharp-cup cyclone to analyze OC and EC concentrations. To remove semi-volatile organic vapors that could potentially be collected onto the quartz filter media, the sampled aerosols were passed through a multichannel, parallel plate denuder with a carbon impregnated filter (CIF) and were collected on a quartz fiber filter. Significant buildup of refractory substances on the filter can occur and promote the catalytic oxidation of carbon on the filter prior to oxygen injection, thereby affecting the accuracy of the analyzer. Therefore, the quartz fiber filter was replaced every 3-5 days by checking the laser correction factor.

Following filtration, the sampled aerosols were iteratively heated at four increasing temperature steps to vaporize organic compounds. Immediately after, the compounds were catalytically oxidized to CO<sub>2</sub> gas over a bed of MnO<sub>2</sub> in the oxidizing oven. The CO<sub>2</sub> gas was swept out of the oxidizing oven under a



stream of high purity (99.999% higher) helium atmosphere and measured by a self-contained non-dispersive infrared detector (NDIR). Following OC oxidation, EC was oxidized to CO<sub>2</sub> when the sample oven temperature is stepped up to 850°C. At the end of every analysis, the semi-continuous OC/EC analyzer was automatically calibrated by injecting a standard CH<sub>4</sub> mixture (5% CH<sub>4</sub> in He). Calibration data, obtained from the known carbon concentration in the loop, were incorporated into every measurement to calculate the analytical results. The NDIR response to the known carbon concentration, as CH<sub>4</sub>, was obtained to determine the NDIR response factor. The precision and the detection limits of the TOT instrument were determined by the variability of the EC and OC concentrations on exposed filters and on filter blanks, respectively. The precision was found to be satisfactory with a relative standard deviation below 5%. The level of EC on the filed blanks was negligible, whereas the OC concentration ranged from 0.1-1.0 µg m<sup>-3</sup>. For a time-resolution of 1 hr. (45 min collection) in this study, the detection limit of the semi-continuous OC/EC analyzer was 0.2 µg m<sup>-3</sup> for OC and 0.04 µg m<sup>-3</sup> for EC.

Concentrations of BC were continuously measured using an Aethalometer (Model AE-31, Magee Scientific Company, USA) which has seven wavelengths (370, 470, 520, 590, 660, 880 and 950 nm). Measurement at 880 nm wavelength is considered as the standard channel to determine BC concentrations because absorption of radiation of other aerosols (e.g. organic aerosols) are negligible at 880 nm (Arnott et al., 2005), and thus was used in the present study. The mass concentrations of PM<sub>2.5</sub> were measured using a Thermo Fisher Scientific TEOM 1405-D since January 2013. Data on hourly concentrations of CO (Thermo 48i) and NO<sub>2</sub> (Thermo 42i), daily SO<sub>2</sub> concentrations (Thermo 43i) at Pudong site (2000-2015), annual average SO<sub>2</sub> concentrations (2000-2014) and emissions (2000-2013) in Shanghai were provided by Pudong Environmental Monitoring Center. The routine QA/QC (quality assurance/quality control) procedures, including the daily zero/standard calibration, span and range check, station environmental control, and staff certification, were followed the Technical Guideline of Automatic Stations of Ambient Air Quality in Shanghai based on the national specification HJ/T193–2005, which was modified from the technical guidance established by the USEPA. The multi-point calibrations were weekly applied upon initial installation of the instruments and the two-point calibrations were applied on a daily basis. Meteorological data, including ambient temperature (*T*), relative humidity (RH), wind direction (WD) and wind speed (WS), were provided by Shanghai

Meteorological Bureau at Century Park station (located around 2 km away from PEMC). All the above online measurement results were averaged to a 1 h resolution.

### 2.3 Satellite data

Satellite-based visible band sensors are capable of detecting atmospheric aerosols and its spatial distribution in a reliable way (van Donkelaar et al., 2010; Martin, 2008). The aerosol optical depth (AOD) is a widely accepted aerosol index retrieved from satellite sensors. Here we use the AOD measured by the moderate resolution imaging spectrometer (MODIS) on-board the Terra satellite to analyze the long-term evolution of aerosol pollution in Shanghai urban areas during the recent decade (2003-2013). Previously, MODIS-derived AOD data had been well validated with the sunphotometer CE318 measurements at 7 sites over the YRD region (including Pudong site in Shanghai; He et al., 2010). Specifically, the MODIS Level 2 aerosol product (MYD04\_3K) was used in this study due to its finer resolution of 3 km and thus greater suitability for providing urban (represented by a 2 km\*2 km square centered at 31.22° N, 121.46° E) data. The AOD values were determined with the dark target algorithm, and only high-quality (quality flag=3) data were retained. Detailed information regarding MODIS-derived AOD data processing has been given elsewhere (Cao et al., 2016).

### 2.4 Source identification

Identifying the presence and characteristics of different sources of air pollution is important if air pollution is to be effectively controlled. Two tools, i.e., the bivariate polar plots (BPP) and the potential source contribution function (PSCF), were used in this study to identify the sources and dispersion characteristics of carbonaceous aerosols in Shanghai. The wind speed (WS) and wind direction (WD) in BPP are measured at near ground level, while the WS and WD in PSCF are calculated at a much higher height (typically 500 m a.g.l). Therefore, BPP is more suitable for tracing the origins of air masses at city scale.

Bivariate polar plots demonstrate how the concentration of a targeted species varies synergistically with wind direction and wind speed in polar coordinates, which have proved to be an effective diagnostic technique for discriminating different emission sources (Carslaw and Ropkins, 2012). To construct BPP, wind speed, wind direction and concentration data are firstly partitioned into wind speed-direction 'bins' and the mean concentration calculated for each bin. We set 10° and 30 for the intervals of wind direction

and wind speed, respectively. Given the inherent wind direction variability in the atmosphere, concentration data with longer time series (e.g., several months in this study) are needed to construct a BPP in order to obtain useful correlations of air concentrations with either wind direction or speed. The two components of wind,  $u$  and  $v$  are calculated through

$$u = \bar{u} \cdot \sin\left(\frac{2\pi}{\theta}\right), v = \bar{u} \cdot \cos\left(\frac{2\pi}{\theta}\right) \quad (1)$$

where  $\bar{u}$  is the mean hourly wind speed and  $\theta$  is the mean wind direction in degrees with  $90^\circ$  as being from the east.

Although a  $u$ ,  $v$ , concentration ( $C$ ) surface can be provided, a better approach is to simulate the surface to describe the concentration as a function of  $u$  and  $v$  so that we can extract the real source features rather than noise. A mathematical framework for fitting a surface is to use a Generalized Additive Model (GAM) (Wood, 2011), expressed as shown in Equation (2):

$$\sqrt{C_i} = \beta_0 + s(u_i, v_i) + \varepsilon_i \quad (2)$$

where  $C_i$  is the  $i^{\text{th}}$  pollutant concentration,  $\beta_0$  is the overall mean of the response,  $s(u_i, v_i)$  is the isotropic smooth function of the  $i^{\text{th}}$  value of covariates  $u$  and  $v$ , and  $\varepsilon_i$  is the  $i^{\text{th}}$  residual. A penalized regression spline was used to model the surface as described by Wood (2011). It should be noted that  $C_i$  is square-root transformed as the transformation generally produces better model diagnostics e.g. normally distributed residuals. Moreover, the smooth function used is isotropic because  $u$  and  $v$  are on the same scales. The isotropic smooth avoids the potential difficulty of smoothing two variables on different scales e.g. wind speed and direction, which introduces further complexities. The methods described above have been made in the R ‘openair’ package and are freely available at [www.openair-project.org](http://www.openair-project.org) (Carslaw and Ropkins, 2012).

The potential source contribution function is a tool essentially based on air mass back trajectory analysis, which has been widely used to estimate the transporting areas of air pollutants over long distances. In this study, the 24 h back trajectories arriving at Pudong Environmental Monitoring Center at a height of 500 m were calculated at 1 h time intervals for each of the four seasons using the NOAA Hybrid Single Particle Lagrangian Integrated Trajectory (HYSPPLIT) model with Global Data Assimilation System

(GDAS) one-degree archive meteorological data (Stein et al., 2015). For each trajectory, it includes a range of latitude-longitude coordinates every 1 h backward in a whole day. If the end point of a trajectory falls into a grid cell  $(i, j)$ , the trajectory is assumed to collect material emitted in the cell (Polissar et al., 1999). The number of end points falling into a single grid cell is  $n_{ij}$ . Some of these trajectory end points are associated with the data with the concentration of aerosol species higher than a threshold value. The number of these points is  $m_{ij}$ . The PSCF then calculates the ratio of  $m_{ij}$  to the total number of points ( $n_{ij}$ ) in the  $ij^{\text{th}}$  grid cell. Higher PSCF values indicate higher potential source contributions to the receptor site. Here the domain for the PSCF was set within the range of (26-42° N, 112.5-125.5° E) in  $0.1^\circ \times 0.1^\circ$  grid cells (Chang et al., 2016). The 75<sup>th</sup> percentile for OC during the four seasons was used as the threshold value  $m_{ij}$ . To reduce the uncertainties of  $m_{ij}/n_{ij}$  for those grid cells with a limited number of points, a weighting function recommended by Polissar et al. (2001) was applied to the PSCF in each season:

$$w_{ij} = \begin{cases} 1.00, 80 < n_{ij} \\ 0.70, 200 < n_{ij} \leq 80 \\ 0.42, 10 < n_{ij} \leq 20 \\ 0.05, n_{ij} \leq 10 \end{cases} \quad (3)$$

### 3 Results and discussions

#### 3.1 Data availability and validation

Between 10 June 2010 and 31 December 2014, the Sunset carbon analyzer was successfully operated during 75% of the time. The original hourly OC and EC concentrations were judged according to the data before and after the measurement event. Outliers of OC and EC were excluded when it was ten times higher than the nearest two-time points. At least two thirds of the data, i.e., 16 hours in a day, 20 days in a month, and 2 months in a season, must be available so that we can calculate the daily, monthly, and seasonal variations, respectively. In this regard, 28490 hourly data in 39250 hours, or 72.6% data availability was reached in the current study. Almost no data were collected in March, April, May, and December 2012, March 2013, and April 2014 due to instrument maintenance and malfunction. Therefore, the monthly variations of OC and EC for these six months and seasonal statistics in 2012 Spring (March, April and May) were not considered.

Four seasons in Shanghai were defined as follows: 1 March-31 May as spring, 1 June-31 August as summer, 1 September-30 November as fall, and 1 December-30 December and 1 January-28 February as winter. The mass concentrations of both EC and BC contribute a similar fraction of the carbonaceous aerosol and are supposed to be comparable. The Aethalometer is one of the most frequently utilized techniques to measure real-time BC mass concentrations, especially for long-term background measurements. In the current study, seasonally different EC concentrations measured by the Sunset OCEC analyzer were validated by comparing with BC data obtained from co-located Aethalometer measurements. The seasonal relationships between Aethalometer BC and Sunset EC are reported in Fig. 2. Slopes ranging from 0.59 to 0.77 are observed with reasonably high correlations ( $r > 0.71$ ). The observed slope indicates that the Aethalometer BC levels were higher than the Sunset EC concentrations. This might be attributed to the fact that the Aethalometer BC is measured and defined differently than the Sunset EC, which is consistent with earlier studies (e.g., Venkatachari et al., 2006). A higher degree of scatter is observed during the Spring compared to the other seasons, suggesting different thermal, optical and chemical behavior during springtime in our study period.

### 3.2 Temporal evolution of OC and EC mass concentrations

#### 3.2.1 Data overview

Summary statistics for the OC and EC concentrations ( $\mu\text{g m}^{-3}$ ) during 10 July 2010-31 December 2014 are presented in Table 1. Taking all data ( $n = 28490$ ) as a whole, hourly concentration levels of OC and EC range from 0.20 to 62.05  $\mu\text{g m}^{-3}$  (average:  $7.19 \pm 4.98 \mu\text{g m}^{-3}$ ) and from 0.06 to 20.49  $\mu\text{g m}^{-3}$  (average:  $2.37 \pm 1.87 \mu\text{g m}^{-3}$ ), respectively, contributing on average ~20% (OC) and ~5.0% (EC) to the  $\text{PM}_{2.5}$  mass between 2013 and 2014. The ratio of OC-to-EC throughout our study period is  $3.70 \pm 1.91$ , which is much high than previous study performed in the Yangtze River Delta region (e.g., 2.36 in Nanjing City (Chen et al., 2017a)). A much higher OC/EC ratio in our study indicates that secondary organic aerosol is more important in Shanghai, which will be extensively discussed in our next work regarding elucidating its sources and formation mechanism.

Figure 3 shows the mass fractions of hourly carbonaceous aerosols classified by  $\text{PM}_{2.5}$  levels during 2013 and 2014. Based on a data sample size of  $n=11790$ , an approximate lognormal distribution is derived for frequency of  $\text{PM}_{2.5}$  concentrations. Among them, 56% and 23% of observed  $\text{PM}_{2.5}$  mass concentrations

exceeded China's first-grade and the second-grade National Ambient Air Quality Standard of  $35 \mu\text{g m}^{-3}$  and  $75 \mu\text{g m}^{-3}$ , respectively, reflecting heavy aerosol pollution in Shanghai. Carbonaceous aerosols contribute a small fraction (22%) of  $\text{PM}_{2.5}$  when  $\text{PM}_{2.5}$  mass concentration greater than  $140 \mu\text{g m}^{-3}$ . However, carbonaceous aerosols dominate the chemical components of  $\text{PM}_{2.5}$  ( $\approx 50\%$ ) when  $\text{PM}_{2.5}$  concentration lower than  $30 \mu\text{g m}^{-3}$ . The result also indicates that the rapid increase in other compounds like inorganic aerosol contributes significantly to heavy haze events in Shanghai, which has also been found in many other cities of China (Huang et al., 2014).

### 3.2.2 Interannual variations

Annually, the OC and EC concentrations (mean  $\pm 1 \sigma$ ) in 2013 ( $8.9 \pm 6.2$  and  $2.6 \pm 2.1 \mu\text{g m}^{-3}$ ,  $n=5547$ ) and 2014 ( $7.8 \pm 4.6$  and  $2.1 \pm 1.6 \mu\text{g m}^{-3}$ ,  $n=6914$ ) were higher than that of 2011 ( $6.3 \pm 4.2$  and  $2.4 \pm 1.8 \mu\text{g m}^{-3}$ ,  $n=8039$ ) and 2012 ( $5.7 \pm 3.8$  and  $2.0 \pm 1.6 \mu\text{g m}^{-3}$ ,  $n=4459$ ). In the first quarter of 2013, China (including Shanghai) experienced extremely severe and persistent haze pollution, with record-high  $\text{PM}_{2.5}$  mass concentrations ( $> 500 \mu\text{g m}^{-3}$ ) and lasting for days or even a month (Zhang et al., 2015b). It seems that previous pollution control policies (Huang et al., 2013; Chen et al., 2014; Normile, 2008) are ineffective. As indicated in Fig. 4, 2013 had the highest frequency with OC (40% of the time) and EC (43% of the time) loadings higher than  $8 \mu\text{g m}^{-3}$  and  $2.5 \mu\text{g m}^{-3}$ , respectively, even though only 41.3% of data was available during January 2013, the most severely polluted month that has been well discussed previously (e.g., Huang et al., 2014; Zhang et al., 2015a). Therefore, a higher carbonaceous aerosol loading in 2013 may be an exception due to the unusually strong influence of haze pollution during wintertime of 2013, which has also been validated previously (Huang et al., 2014).

There is a need to put our study into a longer time frame so that we can obtain a panoramic view of the inter-annual evolution of carbonaceous aerosols levels in Shanghai. Starting from 1999, filter-based measurements of OC and EC were sporadically performed by different groups in Shanghai (SI Table SI), and all these data together with results from our on-line measurements (line-collected circles) were compiled and depicted in Fig. 5a. It is clear that both OC and EC concentrations in Shanghai show a general downtrend during recent decades, suggesting the success of introducing air-cleaning measures such as greater adoption of renewable energy and raising standards for vehicle emissions (Ji et al., 2012; Ke et al., 2017). However, OC and EC monitoring data between 2000 and 2005 were missing, which

make it is impossible to pinpoint the year of transition into a decreasing pattern. More importantly, significant differences (e.g., a factor of two) have been reported for levels of OC and EC when comparing various analytical techniques (Schauer, et al., 2003; Karanasiou, et al., 2015), posing an insurmountable task for us to quantitatively analyze the variations of carbonaceous aerosols and their responses to pollution control measures in Shanghai. As an alternative, we retrieved the AOD data from MODIS satellite in urban and rural Shanghai (Fig. 5b) in order to reproduce the fluctuation of aerosol loading between 2003 and 2013. Figure 4b reinforces a growing consensus that the year of 2006 marked a milestone for Shanghai acting as a pioneer in terms of replacing coal with nature gas. Over 90% of SO<sub>2</sub> emissions in China were derived from coal combustion (Lu et al., 2011), and ambient SO<sub>2</sub> concentrations were directly related to SO<sub>2</sub> emissions. Therefore, the long-term evolution of SO<sub>2</sub> concentration in SI Fig. S2 reflects the process of replacing coal with nature gas in Shanghai. Indeed, energy consumption structure in China, for long stretches, is overwhelmingly dominated by coal despite the fact that PM emissions from natural gas burning can be negligible to a large extent when compared with coal combustion (Hayhoe et al., 2002). Benefitting from China's west-east gas pipeline project (Fig. 1), PM emissions in Shanghai have been cut immensely as there are 7.5 million gas users, including more than 5000 industrial users, and 80% of city taxis are fueled by gas (Hao et al., 2016; Huo et al., 2013). In conclusion, the results from field measurements and satellite observations in Fig. 5 jointly give a "ground truth" that carbonaceous aerosols loading in Shanghai decreased in general from 2006; this was largely driven by the implementation of the clean energy initiative (Lei et al., 2011; Zhao et al., 2013).

### 3.2.3 Monthly and seasonal variations

The hourly, monthly, seasonal, and annual variations of OC and EC concentrations are illustrated in Fig. 6. The monthly average mass concentrations of carbonaceous aerosols show relatively large variations in this study (Fig. 6), with the average value ranging from 4.0 (September 2010) to 15.5 (December 2013)  $\mu\text{g m}^{-3}$  for OC, and from 1.4 (September 2014) to 4.7 (December 2013)  $\mu\text{g m}^{-3}$  for EC (Table 1). The months of September and December presented the lowest (OC: 5.0  $\mu\text{g m}^{-3}$ ; EC: 1.7  $\mu\text{g m}^{-3}$ ) and the highest (OC: 9.7  $\mu\text{g m}^{-3}$ ; EC: 3.5  $\mu\text{g m}^{-3}$ ) average carbonaceous aerosols throughout our study period. This is similar to most cities across China due to a combination of emissions and seasonal variance in meteorology (Cao et al., 2007). Previous work (Chang et al., 2016) show that the month of September in Shanghai has the highest planetary boundary layer (PBL), which favours the vertical dispersion of

ground-emitted pollutants. Besides, higher temperature in September could lead to a shift in the gas-particle equilibrium with more semi-volatile organic compounds (SVOCs) remaining in the gas phase (Yang et al., 2011). In addition, carbonaceous aerosols can also be effectively removed by wet deposition attributed to large amount of precipitation in September (Wang et al., 2006). In contrast, carbonaceous aerosol concentrations elevated in the month of December resulting from relatively stable atmospheric conditions, existence of temperature inversion, and variations in emissions (Feng et al., 2006; Zielinska et al., 2004).

Seasonally, the average concentrations of OC ranged from 5.2 (summer of 2012) to 10.3 (winter of 2014)  $\mu\text{g m}^{-3}$ , and EC ranged from 1.6 (summer of 2012) to 4.0 (winter of 2010)  $\mu\text{g m}^{-3}$ . Except for a slightly higher concentration of EC in the fall of 2012 due to the boost of intensive pollution episodes (indicating by a significantly higher value in P95 or 95<sup>th</sup> percentile; Table 1), higher concentrations of EC were observed in winter for other years, which could be caused by the stagnation of the atmosphere and the stronger influence of regional transport during wintertime (Chen et al., 2017a). However, it is worth noting that the concentration levels of EC in spring, summer and fall were overall similar (Table 1), reflecting a generally local-dominated EC emissions in Shanghai (Cao et al., 2007). As shown in Table 1, there is no uniform pattern for the seasonal variations of OC concentrations, which can be explained by their complexity in terms of the formation processes and sources (see detailed discussion in section 3.2.4 and 3.3). Indeed, in contrast to EC, OC is the mixed product of primary emissions and secondary formation, which could vary significantly in different seasons. In summer, for example, strong solar radiation in summer tends to facilitate photochemical reactions and thus enhance the formation of VOCs to organic aerosols (Tuet et al., 2017; Malecha and Nizkorodov, 2016). Burning of crop residues is also an important source of OC in China (Cheng et al., 2014; Hallquist et al., 2009; Zhang and Cao, 2015), while the burning activities are highly seasonal-dependent and mostly concentrated in fall (Chen et al., 2017b). Cold air masses prevail during winter and early spring, transporting high levels of pollutants (including OC and its precursors emitted from coal-based heating system) from Northern China to the Yangtze River Delta region (Chen et al., 2017a). Scatter plots of OC and EC and their correlation coefficients are shown by season in Fig. 7. Significant correlations ( $R^2 \approx 0.70$ ,  $p < 0.001$ ) between OC and EC were found for winter and fall, indicating that OC and EC share certain similar sources in Shanghai during the two seasons. The highest degree of correlation ( $R^2 = 0.71$ ) was observed during



wintertime when the seasonal OC/EC ratio was the lowest (Table 1), suggesting that primary emissions are an important source contributing to both OC and EC in Shanghai during the cold season (see detailed discussion in section 3.3).

#### 3.2.4 Diurnal variations and weekend-weekday comparisons

5 Diurnal variations of EC concentrations during weekdays and weekends in different seasons of each year are shown in Fig. 8. CO concentrations at Pudong supersite were highly correlated with EC concentrations (Fig. 9). Diurnal variations of OC concentrations during weekdays and weekends in different seasons of each year are shown in Fig. 10, respectively. We first focus on the difference between weekday and weekend patterns. Previously, several short-term studies (e.g., Feng et al., 2009; Stone et al., 2008; Yu et al., 2009; Kim and Hopke, 2008) have observed pronounced differences in the OC and EC patterns between weekdays and weekends, which were thought to be the cycling effects of anthropogenic activities such as vehicular emissions. In Fig. 8, weekday concentrations of EC were 27%, 22%, and 21% higher than the weekend concentrations in the winter of 2011 (the second row from the top and hereafter, the fourth column from the left and hereafter), fall of 2012 (the third row, the second column), and summer of 2013 winter (the fourth row, the fourth column), respectively. We also found that the weekday concentrations of OC in the fall of 2010 (the first row, the third column), fall of 2012 (the third row, the third column) and summer of 2013 (the fourth row, the second column) were 17.8%, 29.7%, and 32.8% higher than that of weekend, respectively (Fig. 10). Nevertheless, our long-term measurement shows that there is no uniform pattern of weekend effect on both OC and EC over the duration of the campaign, suggesting that local sources of carbonaceous aerosols (e.g., on-road traffic) in Shanghai urban center do not vary significantly between weekdays and weekends. To validate our conclusion, we collected traffic flow data (2012-2014) in urban road network from Shanghai Traffic Administration Bureau. SI Fig. S3 shows that average traffic flows in weekends were only around 8% lower than that in weekdays.

20 Distinctive diurnal patterns are observed for EC, generally characterized by two marked peaks occurring at morning (peaking at around 08:00 local time) and during the evening (starting at around 16:00 local time), consistent with the variation of traffic flow in Shanghai (Chang et al., 2012, 2014, 2016). Moreover, as we stated above, CO concentrations were highly correlated with EC concentrations (Fig. 9), indicating

that CO and EC emissions in Shanghai share similar sources (Zhao et al., 2013). Scatter plots of EC vs. CO in Fig. 9 confirms that on-road traffic is a significant source contributing to EC emissions in Shanghai (Chen et al., 2017; Yang et al., 2005).

Relatively flat diurnal cycles were observed for OC during most seasons (Fig. 10). A multi-day build-up of OC was frequently observed during all months (Fig. 4), supporting the notion of regional influences on OC in Shanghai. There was no obvious decrease of OC in the daytime, which might be explained by secondary organic formation. It should be noted that the daytime photochemical production of OC from gas-phase oxidation of VOC might be masked by an elevated planetary boundary layer (PBL). Considering the dilution effect of the PBL height, Sun et al. (2012) found that OC increased gradually from morning to late afternoon, demonstrating the importance of daytime photochemical production of SOA. In this study, OC in fall and winter showed a clear daytime increase until late afternoon, illustrating possible role played by gas-phase photochemical processing in driving the OC diurnal cycle. However, it should be noticed that it is still difficult to pinpoint a specific OC emission source based on our current data. Since ambient OC concentration depends on multiple factors, further study will reveal more information about the different formation mechanisms involved.

Examining the relationship between OC vs. trace gas species ( $\text{NO}_2$  and  $\text{O}_3$ ) could provide more information on the formation and transformation of ambient OC. Since  $\text{NO}_2$  is a major pollutant emitted from combustion processes, its correlation with OC confirms that combustion-generated carbon emissions (including on-road traffic) are important source of OC emissions in Shanghai. OC vs.  $\text{O}_3$  does not show obvious correlation (Fig. 11a). Scatter plots of OC vs.  $\text{NO}_2$  of observations at Pudong supersite show reasonable correlations (Fig. 11b). This finding concurs with the result observed in Mexico City (Yu et al., 2009). First, although  $\text{O}_3$  favour the formation of secondary organic aerosols (SOA), OH radical ( $\text{OH}^\bullet$ )-initiated oxidation may dominate SOA formation, including aqueous-phase oxidation and  $\text{NO}_3$ -radical-initiated nocturnal chemistry. Second, ambient  $\text{O}_3$  concentrations often decreased sharply under high PM loading ( $> 100 \mu\text{g m}^{-3}$ ), which could inhibit SOA formation through  $\text{O}_3$  oxidation (Huang et al., 2014).

### 3.3 Meteorological effects

Figure 12 shows the RH- and  $T$ -dependent distributions of OC and EC mass concentrations throughout the study period. OC show the highest mass loading ( $> 8 \mu\text{g m}^{-3}$ ) at  $T > 30^\circ\text{C}$ , and has no clear dependence on RH. This is coincident with the RH- and  $T$ -dependent distribution pattern of OC/EC (Fig. 12c), which will be used to further investigate the RH/ $T$  impacts on the formation of secondary organic aerosols in future work. Occasionally, high OC mass concentrations can also be found at median and low  $T$  (Fig. 12a), indicating complex sources of OC in Shanghai. For example, there are also several grids with high OC concentrations in the bottom right of Fig. 12a but low OC/EC ratio ( $< 2$ ; Fig. 12c), suggesting the important contribution of primary sources to ambient OC under very low  $T$  ( $< 0^\circ\text{C}$ ) and high RH ( $> 80\%$ ) in Shanghai. At  $-1^\circ\text{C}$ , for instance, the diesel vehicles were estimated to emit 7.6 times more OC than at  $21^\circ\text{C}$  (Zielinska et al., 2004). In contrast to OC, the distribution of EC shows a more obvious concentration gradient as a function of both  $T$  and RH (Fig. 12b), and this is particularly true for WS (Fig. 12d). In Fig. 12b, EC shows the highest mass loading, generally higher than  $3.5 \mu\text{g m}^{-3}$  at  $T < 0^\circ\text{C}$  and RH  $> 80\%$ . This can be explained by the lowest WS (often lower than  $1 \text{ m s}^{-1}$ ; Fig. 12d) occurring under low  $T$  and high RH that tended to accumulate more EC within the city's shallow surface layer (Fig. 12d). In fact, EC and WS demonstrated a generally contrasting RH- and  $T$ -dependent distribution pattern throughout our study period, which strongly indicates that EC variations in Shanghai were WS-dependent.

In Fig. 13a, EC concentrations show more evident WS gradients than OC, with higher concentrations in association with lower wind speeds. This is in line with the conclusion made above that EC concentrations in Shanghai were more sensitive to WS, highlighting the dominating role of local contribution to EC emissions in Shanghai. However, OC and EC in spring did not vary synchronously with WS at low WS ( $< 1 \text{ m s}^{-1}$ ) in the spring, suggesting that regional transport can also be an important source contributing to ambient carbonaceous aerosols in Shanghai. For OC concentrations, their variations in other seasons were also not strictly followed WS gradients, confirming that the share of regional transport contribution to ambient OC was comparable with local sources in Shanghai.

In Fig. 13b, both OC and EC show clear wind sector gradients, with higher concentrations in association with winds from the southwest (SW) and west (W), and lower concentrations with east (E) and northeast

(NE) wind. The average mass concentrations of OC and EC from the SW were  $9.8 \mu\text{g m}^{-3}$  and  $3.4 \mu\text{g m}^{-3}$ , respectively, which were  $\sim 1.7$  times than that from the NE ( $5.9 \mu\text{g m}^{-3}$  and  $1.9 \mu\text{g m}^{-3}$  for OC and EC, respectively). This can be explained by the high WS (often larger than  $6 \text{ m s}^{-1}$ ; Fig. 14) from the E and NE associated with clean air masses from remote oceans (SI Fig. S1) while low WS (often lower than  $6 \text{ m s}^{-1}$ ; Fig. 14) from the W and SW is associated with polluted air masses from inner Shanghai or inland China (SI Fig. S1). Overall, OC and EC increased as wind sectors changed along the NE-E-SE-S-SW gradient, and then decreased along the SW-W-NW-N gradient (Fig. 13). Such wind sector dependence of carbonaceous aerosols is generally consistent with the spatial distribution of  $\text{PM}_{2.5}$  in Shanghai and its neighbouring regions (Ma et al., 2014). However, this study identified that winds from the SW were the most important pathway of contributing ambient carbonaceous aerosols from inland China to Shanghai. This result is different from most previous studies which concluded that the NW or N in Northern China were the dominant source region of coal-related aerosol species (such as sulfate) and gases (such as  $\text{SO}_2$ ).

Seasonal bivariate polar plots (BPP) of EC concentrations for 2010-2014 are shown in Fig. 14, and the distribution pattern generally agrees with OC (SI Fig. S4). There are several points that should be noted. First, higher EC mass loadings ( $> 3 \mu\text{g m}^{-3}$ ) but lower OC/EC ratios ( $< 3$ ; SI Fig. S5) near the field site (indicating by  $\text{WS} < 2 \text{ m s}^{-1}$ ) are seen as a characteristic feature for every season throughout the sampling period, suggesting that local and primary emissions (e.g., on-road traffic) are a stable and important source contributing to ambient EC concentrations in Shanghai. Second, Shanghai's main urban districts are southwest of the field site (SI Fig. S1). Fig. 13b and Fig. 14 jointly identify that winds from the SW consistently had the highest EC concentrations. Given the relatively low WS ( $< 6 \text{ m s}^{-1}$  in most cases; Fig. 14) in the SW (where the main urban districts located), the urban areas of Shanghai were highly likely the major source areas for EC. Thirdly, EC also displayed relatively high concentrations in the NW during winter and spring, and the lowest in the E and SE during summer and fall (Fig. 14). In fact, Shanghai has a subtropical monsoon climate and is bounded to the east by the East China Sea (SI Fig. S1). Winters and springs in Shanghai are chilly, with northwesterly winds from Siberia transporting high levels of air pollutants in Northern China to the YRD region resulting in poor air quality in Shanghai. Conversely, the SE winds originating from the East China sea prevail in summers and fall. Moreover, the city is susceptible to typhoons in summer and the beginning of fall, thus carbonaceous aerosols can be effectively removed by wet deposition attributed to large amount of rainfall (Huang et al., 2008).

As shown in Fig. 15, the OC concentrations in Shanghai also have potential source areas in common. There is a pollution transport belt along the middle and lower reaches of the Yangtze River among the four seasons, which can be attributed to two main reasons. First, there are five important rice-growing areas (of a total of nine in China), i.e., the Jiangnan Plain in Hubei Province, Dongting Lake Plain in Hunan Province, Poyang Lake Plain in Jiangxi Province, Yangtze-Huaihe area in Anhui and Jiangsu Province, and Taihu Lake Plain in Jiangsu Province are under the pollution transport belt (SI Fig. S1). Previously, field measurements, model simulations and satellite observations have identified that inter-province transport of air pollutants emitted from un-prescribed biomass (mainly rice residues) burning was an important source of air pollution throughout the YRD region. For example, based on ambient monitoring data and the WRF/CMAQ (Weather Research and Forecasting (WRF) and Community Multiscale Air Quality (CMAQ)) model simulation during the beginning of summer in 2011, Cheng et al. (2014) showed that biomass burning contributed 37% of PM<sub>2.5</sub>, 70% of OC and 61% of EC in five cities (including Shanghai) of the YRD region. Moreover, it is estimated that the PM<sub>2.5</sub> exposure level could be reduced by 47% for the YRD region if complete biomass burning was forbidden and a significant health benefit would be expected (Cheng et al., 2014). Nevertheless, biomass burning activities are mostly concentrated in the months of June and October, the periods of crop post-harvest. The second but more important reason could be the influence of anthropogenic activities (excluding prescribed biomass burning; Chen et al., 2017a). Indeed, the pollution belt overlaps the Yangtze River Economic Belt, one of China's most densely populated areas clustering with many cities (including big cities like Wuhan, Changsha, Nanchang, Hefei, Nanjing, and Suzhou) and numerous industrial complexes (including massive petrochemical, iron and steel, and chemical processing industry). In brief, our PSCF analysis highlighted the importance of long-range transport contributing to OC pollution in Shanghai.

#### 4 Conclusions

This paper presents the results from a multi-year and near real-time measurement study of carbonaceous aerosols in PM<sub>2.5</sub> using a Sunset semi-continuous OC/EC analyser, conducted at an urban supersite in Shanghai from July 2010 to December 2014. The annual mass concentrations of OC (EC) from 2011 to 2014 were  $6.3 \pm 4.2$  ( $2.4 \pm 1.8$ ),  $5.7 \pm 3.8$  ( $2.0 \pm 1.6$ ),  $8.9 \pm 6.2$  ( $2.6 \pm 2.1$ ), and  $7.8 \pm 4.6$  ( $2.1 \pm 1.6$ )  $\mu\text{g m}^{-3}$ ,

respectively, accounting for 13.2-24.6% (3.9-6.6%) of  $PM_{2.5}$  mass. We integrated the results from historical field measurements and satellite observations, concluding that carbonaceous aerosol pollution in Shanghai has gradually reduced since 2006. Our results confirm the success of replacing coal with cleaner energy such as natural gas in Shanghai, which can be adopted in other megacities like Beijing and Guangzhou to curb  $PM_{2.5}$  pollution.

Both OC and EC showed concentration gradients as a function of wind direction and wind speed, generally with higher values associated with winds from the southwest, west, and northwest. This was consistent with their higher potential as source areas, as determined by the potential source contribution function analysis. A common high potential source area, located along the middle and lower reaches of the Yangtze River instead of Northern China, was pinpointed during all seasons. The results of this study also highlighted that the reduction of biomass burning and anthropogenic emissions for the YRD region requires regional joint management and control strategies.

## 5 Data availability

Data are available from the corresponding authors on request. The authors prefer not to publish the data at the present stage in order to avoid compromising the future of ongoing publications.

*Acknowledgements.* This study was supported by the National Key Research and Development Program of China (2017YFC0210100), National Science Foundation of China (Grant nos. 91644103 and 41603104). Yunhua Chang and Zhong Zou acknowledge the support of the Start-up Foundation for Introducing Talent to NUIST and Shanghai Pudong New Area Sci-tech Development Funds (Grant no. PKJ2016-C01), respectively. We also acknowledge the Qingyue Open Environmental Data Centre (<http://data.epmap.org>) for the unconditional help in terms of providing criteria pollutants monitoring data.

## References

- Arhami, M., Kuhn, T., Fine, P. M., Delfino, R. J., and Sioutas, C.: Effects of sampling artifacts and operating parameters on the performance of a semicontinuous particulate elemental carbon/organic carbon monitor, *Environ. Sci. Technol.*, 40, 945-954, doi: 10.1021/es0510313, 2006.
- 5 Arnott, W. P., Hamasha, K., W. Moosmüller, H., Sheridan, P. J., and Ogren, J. A., Towards aerosol light-absorption measurements with a 7-wavelength Aethalometer: Evaluation with a photoacoustic instrument and 3-wavelength Nephelometer, *Aerosol Sci. Technol.*, 39, 17-29, doi: 10.1080/027868290901972, 2005.
- Bond, T. C., Doherty, S. J., Fahey, D., Forster, P., Berntsen, T., DeAngelo, B., Flanner, M., Ghan, S.,  
10 Kärcher, B., and Koch, D.: Bounding the role of black carbon in the climate system: A scientific assessment, *J. Geophys. Res.*, 118, 5380-5552, doi: 10.1002/jgrd.50171, 2013.
- Cao, C., Lee, X., Liu, S., Schultz, N., Xiao, W., Zhang, M., and Zhao, L.: Urban heat islands in China enhanced by haze pollution, *Nat. Commun.*, 7, 12509, doi: 10.1038/ncomms12509, 2016.
- Cao, G., Zhang, X., and Zheng, F.: Inventory of black carbon and organic carbon emissions from China,  
15 *Atmos. Environ.*, 40, 6516-6527, doi: 10.1016/j.atmosenv.2006.05.070, 2006.
- Cao, J. J., Wang, Q. Y., Chow, J. C., Watson, J. G., Tie, X. X., Shen, Z. X., Wang, P., and An, Z. S.: Impacts of aerosol compositions on visibility impairment in Xi'an, China, *Atmos. Environ.*, 59, 559-566, doi: 10.1016/j.atmosenv.2012.05.036, 2012.
- Cao, J. J., Lee, S. C., Ho, K. F., Zou, S. C., Fung, K., Li, Y., Watson, J. G., and Chow, J. C.: Spatial and  
20 seasonal variations of atmospheric organic carbon and elemental carbon in Pearl River Delta Region, China, *Atmos. Environ.*, 38, 4447-4456, doi: 10.1016/j.atmosenv.2004.05.016, 2004.
- Cao, J. J., Wu, F., Chow, J. C., Lee, S. C., Li, Y., Chen, S. W., An, Z. S., Fung, K. K., Watson, J. G., Zhu, C. S., and Liu, S. X.: Characterization and source apportionment of atmospheric organic and elemental carbon during fall and winter of 2003 in Xi'an, China, *Atmos. Chem. Phys.*, 5, 3127-3137,  
25 doi: 10.5194/acp-5-3127-2005, 2005.
- Cao, J. J., Lee, S. C., Chow, J. C., Watson, J. G., Ho, K. F., Zhang, R. J., Jin, Z. D., Shen, Z. X., Chen, G. C., Kang, Y. M., Zou, S. C., Zhang, L. Z., Qi, S. H., Dai, M. H., Cheng, Y., and Hu, K.: Spatial and seasonal distributions of carbonaceous aerosols over China, *J. Geophys. Res.*, 112, doi: 10.1029/2006JD008205, 2007.
- 30 Cao, J. J., Zhu, C. S., Tie, X. X., Geng, F. H., Xu, H. M., Ho, S. S. H., Wang, G. H., Han, Y. M., and Ho, K. F.: Characteristics and sources of carbonaceous aerosols from Shanghai, China, *Atmos. Chem. Phys.*, 13, 803-817, doi: 10.5194/acp-13-803-2013, 2013.
- Carlsaw, D. C., and Ropkins, K.: openair-An R package for air quality data analysis, *Environ. Modell. Softw.*, 27-28, 52-61, doi: 10.1016/j.envsoft.2011.09.008, 2012.
- 35 Castro, L. M., Pio, C. A., Harrison, R. M., and Smith, D. J. T.: Carbonaceous aerosol in urban and rural European atmospheres: estimation of secondary organic carbon concentrations, *Atmos. Environ.*, 33, 2771-2781, doi: 10.1016/S1352-2310(98)00331-8, 1999.
- Chang, Y.: China needs a tighter PM<sub>2.5</sub> limit and a change in priorities, *Environ. Sci. Technol.*, 46, 7069-7070, doi: 10.1021/es3022705, 2012.
- 40 Chang, Y., Zou, Z., Deng, C., Huang, K., Collett, J. L., Lin, J., and Zhuang, G.: The importance of vehicle emissions as a source of atmospheric ammonia in the megacity of Shanghai, *Atmos. Chem. Phys.*, 16, 3577-3594, doi: 10.5194/acp-16-3577-2016, 2016
- Chang, Y. H.: Non-agricultural ammonia emissions in urban China, *Atmos. Chem. Phys. Discuss.*, 14, 8495-8531, doi: 10.5194/acpd-14-8495-2014, 2014.

- Chen, D., Cui, H., Zhao, Y., Yin, L., Lu, Y., and Wang, Q.: A two-year study of carbonaceous aerosols in ambient PM<sub>2.5</sub> at a regional background site for western Yangtze River Delta, China, *Atmos. Res.*, 183, 351-361, doi: 10.1016/j.atmosres.2016.09.004, 2017a.
- Chen, J., Li, C., Ristovski, Z., Milic, A., Gu, Y., Islam, M. S., Wang, S., Hao, J., Zhang, H., He, C., Guo, H., Fu, H., Miljevic, B., Morawska, L., Thai, P., Lam, Y. F., Pereira, G., Ding, A., Huang, X., and Dumka, U. C.: A review of biomass burning: Emissions and impacts on air quality, health and climate in China, *Sci. Total Environ.*, 579, 1000-1034, doi: 10.1016/j.scitotenv.2016.11.025, 2017b.
- Chen, K., Yin, Y., Kong, S., Xiao, H., Wu, Y., Chen, J., and Li, A.: Size-resolved chemical composition of atmospheric particles during a straw burning period at Mt. Huang (the Yellow Mountain) of China, *Atmos. Environ.*, 84, 380-389, doi: 10.1016/j.atmosenv.2013.11.040, 2014.
- Cheng, Y., He, K. B., Duan, F. K., Zheng, M., Ma, Y. L., and Tan, J. H.: Positive sampling artifact of carbonaceous aerosols and its influence on the thermal-optical split of OC/EC, *Atmos. Chem. Phys.*, 9, 7243-7256, doi: 10.5194/acp-9-7243-2009, 2009.
- Cheng, Z., Wang, S., Fu, X., Watson, J. G., Jiang, J., Fu, Q., Chen, C., Xu, B., Yu, J., Chow, J. C., and Hao, J.: Impact of biomass burning on haze pollution in the Yangtze River delta, China: A case study in summer 2011, *Atmos. Chem. Phys.*, 14, 4573-4585, 10.5194/acp-14-4573-2014, 2014.
- China Automotive Industry Yearbook, ISBN/ISSN: CN12--1228/U, 2014. (In Chinese)
- Cui, H., Mao, P., Zhao, Y., Nielsen, C. P., and Zhang, J.: Patterns in atmospheric carbonaceous aerosols in China: Emission estimates and observed concentrations, *Atmos. Chem. Phys.*, 15, 8657-8678, doi: 10.5194/acp-15-8657-2015, 2015.
- Duan, F., He, K., Ma, Y., Jia, Y., Yang, F., Lei, Y., Tanaka, S., and Okuta, T.: Characteristics of carbonaceous aerosols in Beijing, China, *Chemosphere*, 60, 355-364, doi: 10.1016/j.chemosphere.2004.12.035, 2005.
- Duan, J., Tan, J., Cheng, D., Bi, X., Deng, W., Sheng, G., Fu, J., and Wong, M. H.: Sources and characteristics of carbonaceous aerosol in two largest cities in Pearl River Delta Region, China, *Atmos. Environ.*, 41, 2895-2903, doi: 10.1016/j.atmosenv.2006.12.017, 2007.
- Fang, C., Li, G., and Wang, S.: Changing and differentiated urban landscape in China: Spatiotemporal patterns and driving forces, *Environ. Sci. Technol.*, 50, 2217-2227, doi: 10.1021/acs.est.5b05198, 2016.
- Feng, J., Hu, M., Chan, C. K., Lau, P. S., Fang, M., He, L., and Tang, X.: A comparative study of the organic matter in PM<sub>2.5</sub> from three Chinese megacities in three different climatic zones, *Atmos. Environ.*, 40, 3983-3994, doi: 10.1016/j.atmosenv.2006.02.017, 2006.
- Feng, Y., Chen, Y., Guo, H., Zhi, G., Xiong, S., Li, J., Sheng, G., and Fu, J.: Characteristics of organic and elemental carbon in PM<sub>2.5</sub> samples in Shanghai, China, *Atmos. Res.*, 92, 434-442, doi: 10.1016/j.atmosres.2009.01.003, 2009.
- Fu, T. M., Cao, J. J., Zhang, X. Y., Lee, S. C., Zhang, Q., Han, Y. M., Qu, W. J., Han, Z., Zhang, R., Wang, Y. X., Chen, D., and Henze, D. K.: Carbonaceous aerosols in China: Top-down constraints on primary sources and estimation of secondary contribution, *Atmos. Chem. Phys.*, 12, 2725-2746 doi: 10.5194/acp-12-2725-2012, 2012.
- Gustafsson, Ö., Kruså, M., Zencak, Z., Sheesley, R. J., Granat, L., Engström, E., Praveen, P. S., Rao, P. S. P., Leck, C., and Rodhe, H.: Brown clouds over South Asia: Biomass or fossil fuel combustion?, *Science*, 323, 495-498, doi: 10.1126/science.1164857, 2009.
- Hallquist, M., Wenger, J. C., Baltensperger, U., Rudich, Y., Simpson, D., Claeys, M., Dommen, J., Donahue, N. M., George, C., Goldstein, A. H., Hamilton, J. F., Herrmann, H., Hoffmann, T., Iinuma,



- Y., Jang, M., Jenkin, M. E., Jimenez, J. L., Kiendler-Scharr, A., Maenhaut, W., McFiggans, G., Mentel, T. F., Monod, A., Prévôt, A. S. H., Seinfeld, J. H., Surratt, J. D., Szmigielski, R., and Wildt, J.: The formation, properties and impact of secondary organic aerosol: Current and emerging issues, *Atmos. Chem. Phys.*, 9, 5155-5236, doi: 10.5194/acp-9-5155-2009, 2009.
- 5 Hao, H., Liu, Z., Zhao, F., and Li, W.: Natural gas as vehicle fuel in China: A review, *Renew. Sust. Energ. Rev.*, 62, 521-533, doi: 10.1016/j.rser.2016.05.015, 2016.
- Hayhoe, K., Kheshgi, H. S., Jain, A. K., and Wuebbles, D. J.: Substitution of natural gas for coal: Climatic effects of utility sector emissions, *Climatic Change*, 54, 107-139, doi: 10.1023/a:1015737505552, 2002.
- 10 He, K., Yang, F., Ma, Y., Zhang, Q., Yao, X., Chan, C. K., Cadle, S., Chan, T., and Mulawa, P.: The characteristics of PM<sub>2.5</sub> in Beijing, China, *Atmos. Environ.*, 35, 4959-4970, doi: 10.1016/S1352-2310(01)00301-6, 2001.
- He, Q., Li, C., Tang, X., Li, H., Geng, F., and Wu, Y.: Validation of MODIS derived aerosol optical depth over the Yangtze River Delta in China, *Remote Sens. Environ.*, 114, 1649-1661, doi: 10.1016/j.rse.2010.02.015, 2010.
- 15 Huang, C., Chen, C. H., Li, L., Cheng, Z., Wang, H. L., Huang, H. Y., Streets, D. G., Wang, Y. J., Zhang, G. F., and Chen, Y. R.: Emission inventory of anthropogenic air pollutants and VOC species in the Yangtze River Delta region, China, *Atmos. Chem. Phys.*, 11, 4105-4120, doi: 10.5194/acp-11-4105-2011, 2011.
- 20 Huang, K., Zhuang, G., Xu, C., Wang, Y., and Tang, A.: The chemistry of the severe acidic precipitation in Shanghai, China, *Atmos. Res.*, 89, 149-160, doi: 10.1016/j.atmosres.2008.01.006, 2008.
- Huang, K., Zhuang, G., Lin, Y., Wang, Q., Fu, J. S., Fu, Q., Liu, T., and Deng, C.: How to improve the air quality over megacities in China: pollution characterization and source analysis in Shanghai before, during, and after the 2010 World Expo, *Atmos. Chem. Phys.*, 13, 5927-5942, doi: 10.5194/acp-13-5927-2013, 2013.
- 25 Huang, R. J., Zhang, Y., Bozzetti, C., Ho, K. F., Cao, J. J., Han, Y., Daellenbach, K. R., Slowik, J. G., Platt, S. M., Canonaco, F., Zotter, P., Wolf, R., Pieber, S. M., Brun, E. A., Crippa, M., Ciarelli, G., Piazzalunga, A., Schwikowski, M., Abbazade, G., Schnelle-Kreis, J., Zimmermann, R., An, Z., Szidat, S., Baltensperger, U., El Haddad, I., and Prevot, A. S.: High secondary aerosol contribution to particulate pollution during haze events in China, *Nature*, 514, 218-222, doi: 10.1038/nature13774, 2014.
- 30 Huo, H., Zhang, Q., Liu, F., and He, K.: Climate and environmental effects of electric vehicles versus compressed natural gas vehicles in China: A life-cycle analysis at provincial level, *Environ. Sci. Technol.*, 47, 1711-1718, doi: 10.1021/es303352x, 2013.
- 35 Jacobson, M. Z.: Strong radiative heating due to the mixing state of black carbon in atmospheric aerosols, *Nature*, 409, 695-697, doi: 10.1038/35055518, 2001.
- Ji, S., Cherry, C. R., M, J. B., Wu, Y., and Marshall, J. D.: Electric vehicles in China: emissions and health impacts, *Environ. Sci. Technol.*, 46, 2018-2024, doi: 10.1021/es202347q, 2012.
- Karanasiou, A., Minguillón, M. C., Viana, M., Alastuey, A., Putaud, J. P., Maenhaut, W., Panteliadis, P., Močnik, G., Favez, O., and Kuhlbusch, T. A. J.: Thermal-optical analysis for the measurement of elemental carbon (EC) and organic carbon (OC) in ambient air a literature review, *Atmos. Meas. Tech. Discuss.*, 8, 9649-9712, doi: 10.5194/amtd-8-9649-2015, 2015.
- 40

- Ke, W., Zhang, S., Wu, Y., Zhao, B., Wang, S., and Hao, J.: Assessing the future vehicle fleet electrification: The impacts on regional and urban air quality, *Environ. Sci. Technol.*, 51, 1007-1016, doi: 10.1021/acs.est.6b04253, 2017.
- Kim, E., and Hopke, P. K.: Source characterization of ambient fine particles at multiple sites in the Seattle area, *Atmos. Environ.*, 42, 6047-6056, doi: 10.1016/j.atmosenv.2008.03.032, 2008.
- Klimont, Z., Cofala, J., Xing, J., Wei, W., Zhang, C., Wang, S., Kejun, J., Bhandari, P., Mathur, R., Purohit, P., Rafaj, P., Chambers, A., Amann, M., and Hao, J.: Projections of SO<sub>2</sub>, NO<sub>x</sub> and carbonaceous aerosols emissions in Asia, *Tellus B*, 61, 602-617, doi: 10.1111/j.1600-0889.2009.00428.x, 2009.
- Lei, Y., Zhang, Q., He, K. B., and Streets, D. G.: Primary anthropogenic aerosol emission trends for China, 1990-2005, *Atmos. Chem. Phys.*, 11, 931-954, doi: 10.5194/acp-11-931-2011, 2011.
- Li, M., Zhang, Q., Kurokawa, J., Woo, J. H., He, K. B., Lu, Z., Ohara, T., Song, Y., Streets, D. G., Carmichael, G. R., Cheng, Y. F., Hong, C. P., Huo, H., Jiang, X. J., Kang, S. C., Liu, F., Su, H., and Zheng, B.: MIX: a mosaic Asian anthropogenic emission inventory for the MICS-Asia and the HTAP projects, *Atmos. Chem. Phys. Discuss.*, 2015, 34813-34869, 10.5194/acpd-15-34813-2015, 2015.
- Li, X., Wang, S., Duan, L., Hao, J., and Nie, Y.: Carbonaceous aerosol emissions from household biofuel combustion in China, *Environ. Sci. Technol.*, 43, 6076-6081, doi: 10.1021/es803330j, 2009.
- Lim, S. S., Vos, T., Flaxman, A. D., Danaei, G., Shibuya, K., Adair-Rohani, H., AlMazroa, M. A., Amann, M., Anderson, H. R., Andrews, K. G., Aryee, M., Atkinson, C., Bacchus, L. J., Bahalim, A. N., Balakrishnan, K., Balmes, J., Barker-Collo, S., Baxter, A., Bell, M. L., Blore, J. D., Blyth, F., Bonner, C., Borges, G., Bourne, R., Boussinesq, M., Brauer, M., Brooks, P., Bruce, N. G., Brunekreef, B., Bryan-Hancock, C., Bucello, C., Buchbinder, R., Bull, F., Burnett, R. T., Byers, T. E., Calabria, B., Carapetis, J., Carnahan, E., Chafe, Z., Charlson, F., Chen, H., Chen, J. S., Cheng, A. T.-A., Child, J. C., Cohen, A., Colson, K. E., Cowie, B. C., Darby, S., Darling, S., Davis, A., Degenhardt, L., Dentener, F., Des Jarlais, D. C., Devries, K., Dherani, M., Ding, E. L., Dorsey, E. R., Driscoll, T., Edmond, K., Ali, S. E., Engell, R. E., Erwin, P. J., Fahimi, S., Falder, G., Farzadfar, F., Ferrari, A., Finucane, M. M., Flaxman, S., Fowkes, F. G. R., Freedman, G., Freeman, M. K., Gakidou, E., Ghosh, S., Giovannucci, E., Gmel, G., Graham, K., Grainger, R., Grant, B., Gunnell, D., Gutierrez, H. R., Hall, W., Hoek, H. W., Hogan, A., Hosgood Iii, H. D., Hoy, D., Hu, H., Hubbell, B. J., Hutchings, S. J., Ibeanusi, S. E., Jacklyn, G. L., Jasrasaria, R., Jonas, J. B., Kan, H., Kanis, J. A., Kassebaum, N., Kawakami, N., Khang, Y.-H., Khatibzadeh, S., Khoo, J.-P., Kok, C., Laden, F., Lalloo, R., Lan, Q., Lathlean, T., Leasher, J. L., Leigh, J., Li, Y., Lin, J. K., Lipshultz, S. E., London, S., Lozano, R., Lu, Y., Mak, J., Malekzadeh, R., Mallinger, L., Marcenes, W., March, L., Marks, R., Martin, R., McGale, P., McGrath, J., Mehta, S., Memish, Z. A., Mensah, G. A., Merriman, T. R., Micha, R., Michaud, C., Mishra, V., Hanafiah, K. M., Mokdad, A. A., Morawska, L., Mozaffarian, D., Murphy, T., Naghavi, M., Neal, B., Nelson, P. K., Nolla, J. M., Norman, R., Olives, C., Omer, S. B., Orchard, J., Osborne, R., Ostro, B., Page, A., Pandey, K. D., Parry, C. D. H., Passmore, E., Patra, J., Pearce, N., Pelizzari, P. M., Petzold, M., Phillips, M. R., Pope, D., Pope Iii, C. A., Powles, J., Rao, M., Razavi, H., Rehfues, E. A., Rehm, J. T., Ritz, B., Rivara, F. P., Roberts, T., Robinson, C., Rodriguez-Portales, J. A., Romieu, I., Room, R., Rosenfeld, L. C., Roy, A., Rushton, L., Salomon, J. A., Sampson, U., Sanchez-Riera, L., Sanman, E., Sapkota, A., Seedat, S., Shi, P., Shield, K., Shivakoti, R., Singh, G. M., Sleet, D. A., Smith, E., Smith, K. R., Stapelberg, N. J. C., Steenland, K., Stöckl, H., Stovner, L. J., Straif, K., Straney, L., Thurston, G. D., Tran, J. H.,

- Van Dingenen, R., van Donkelaar, A., Veerman, J. L., Vijayakumar, L., Weintraub, R., Weissman, M. M., White, R. A., Whiteford, H., Wiersma, S. T., Wilkinson, J. D., Williams, H. C., Williams, W., Wilson, N., Woolf, A. D., Yip, P., Zielinski, J. M., Lopez, A. D., Murray, C. J. L., and Ezzati, M.: A comparative risk assessment of burden of disease and injury attributable to 67 risk factors and risk factor clusters in 21 regions, 1990–2010: a systematic analysis for the Global Burden of Disease Study 2010, *Lancet*, 380, 2224–2260, doi: 10.1016/S0140-6736(12)61766-8, 2012.
- 5 Lin, J., Pan, D., Davis, S. J., Zhang, Q., He, K., Wang, C., Streets, D. G., Wuebbles, D. J., and Guan, D.: China's international trade and air pollution in the United States, *Proc. Natl. Acad. Sci. U.S.A.*, 111, doi: 1736-1741, 10.1073/pnas.1312860111, 2014.
- 10 Lu, Z., Zhang, Q., and Streets, D. G.: Sulfur dioxide and primary carbonaceous aerosol emissions in China and India, 1996–2010, *Atmos. Chem. Phys.*, 11, 9839–9864, doi: 10.5194/acp-11-9839-2011, 2011.
- Ma, Z., Hu, X., Huang, L., Bi, J., and Liu, Y.: Estimating ground-level PM<sub>2.5</sub> in China using satellite remote sensing, *Environ. Sci. Technol.*, 48, 7436–7444, doi: 10.1021/es5009399, 2014.
- 15 Malecha, K. T., and Nizkorodov, S. A.: Photodegradation of secondary organic aerosol particles as a source of small, oxygenated volatile organic compounds, *Environ. Sci. Technol.*, 50, 9990–9997, doi: 10.1021/acs.est.6b02313, 2016.
- Martin, R. V.: Satellite remote sensing of surface air quality, *Atmos. Environ.*, 42, 7823–7843, doi: 10.1016/j.atmosenv.2008.07.018, 2008.
- 20 MEP (P.R.C Ministry of Environmental Protection): The state council issues action plan on prevention and control of air pollution introducing ten measures to improve air quality, [http://english.mep.gov.cn/News\\_service/infocus/201309/t20130924\\_260707.htm](http://english.mep.gov.cn/News_service/infocus/201309/t20130924_260707.htm), 2013. Accessible: Feb. 20, 2016.
- NIOSH: Elemental Carbon (Diesel Particulate): Method 5040, in: NIOSH Manual of Analytical Methods, 25 4th edition, edited by: Eller, P. M. and Cassinelli, M. E., National Institute for Occupational Safety and Health, DHHS (NIOSH), Cincinnati, OH, USA, Publication No. 96-135, 1996.
- Normile, D.: China's living laboratory in urbanization, *Science*, 319, 740–743, doi: 10.1126/science.319.5864.740, 2008.
- Park, R. J., Jacob, D. J., Chin, M., and Martin, R. V.: Sources of carbonaceous aerosols over the United States and implications for natural visibility, *J. Geophys. Res.*, 108, doi: 10.1029/2002JD003190, 30 2003.
- Polissar, A. V., Hopke, P. K., Paatero, P., Kaufmann, Y. J., Hall, D. K., Bodhaine, B. A., Dutton, E. G., and Harris, J. M.: The aerosol at Barrow, Alaska: Long-term trends and source locations, *Atmos. Environ.*, 33, 2441–2458, doi: 10.1016/S1352-2310(98)00423-3, 1999.
- 35 Polissar, A. V., Hopke, P. K., and Harris, J. M.: Source Regions for Atmospheric Aerosol Measured at Barrow, Alaska, *Environ. Sci. Technol.*, 35, 4214–4226, doi: 10.1021/es0107529, 2001.
- Pope III, C. A., Burnett, R. T., Thun, M. J., Calle, E. E., Krewski, D., Ito, K., and Thurston, G. D.: Lung cancer, cardiopulmonary mortality, and long-term exposure to fine particulate air pollution, *JAMA: J. Am Med. Assoc.*, 287, 1132–1141, 2002.
- 40 Qiao, L., Cai, J., Wang, H., Wang, W., Zhou, M., Lou, S., Chen, R., Dai, H., Chen, C., and Kan, H.: PM<sub>2.5</sub> constituents and hospital emergency-room visits in Shanghai, China, *Environ. Sci. Technol.*, 48, doi: 10406-10414, 10.1021/es501305k, 2014.
- Samet, J. M., Dominici, F., Currier, I., Coursac, I., and Zeger, S. L.: Fine particulate air pollution and mortality in 20 US cities, 1987–1994, *New Engl. J. Med.*, 343, 1742–1749, 2000.

- Schauer, J. J., Mader, B. T., Deminter, J. T., Heidemann, G., Bae, M., Seinfeld, J., Flagan, R., Cary, R., Smith, D., Huebert, B., Bertram, T., Howell, S., Kline, J., Quinn, P., Bates, T., Turpin, B., Lim, H., Yu, J., Yang, H., and Keywood, M.: ACE-Asia intercomparison of a thermal-optical method for the determination of particle-phase organic and elemental carbon, *Environ. Sci. Technol.*, 37(5): 993-1001, doi: 10.1021/es020622f, 2003.
- Seinfeld, J. H., and Pandis, S. N.: *Atmospheric chemistry and physics: From air pollution to climate change*, John Wiley & Sons, 2006.
- Sun, Y. L., Wang, Z. F., Du, W., Zhang, Q., Wang, Q. Q., Fu, P. Q., Pan, X. L., Li, J., Jayne, J., and Worsnop, D. R.: Long-term real-time measurements of aerosol particle composition in Beijing, China: seasonal variations, meteorological effects, and source analysis, *Atmos. Chem. Phys.*, doi: 15, 10149-10165, 10.5194/acp-15-10149-2015, 2015.
- Stein, A. F., Draxler, R. R., Rolph, G. D., Stunder, B. J. B., Cohen, M. D., and Ngan, F.: NOAA's HYSPLIT atmospheric transport and dispersion modeling system, *B. Am. Meteorol. Soc.*, 96, 2059-2077, doi: 10.1175/bams-d-14-00110.1, 2015.
- Stone, E. A., Snyder, D. C., Sheesley, R. J., Sullivan, A. P., Weber, R. J., and Schauer, J. J.: Source apportionment of fine organic aerosol in Mexico City during the MILAGRO experiment 2006, *Atmos. Chem. Phys.*, 8, 1249-1259, doi: 10.5194/acp-8-1249-2008, 2008.
- Tuet, W. Y., Chen, Y., Xu, L., Fok, S., Gao, D., Weber, R. J., and Ng, N. L.: Chemical oxidative potential of secondary organic aerosol (SOA) generated from the photooxidation of biogenic and anthropogenic volatile organic compounds, *Atmos. Chem. Phys.*, 17, 839-853, doi: 10.5194/acp-17-839-2017, 2017.
- Turpin, B. J., and Huntzicker, J. J.: Secondary formation of organic aerosol in the Los Angeles basin: A descriptive analysis of organic and elemental carbon concentrations, *Atmos. Environ.*, 25, 207-215, doi: 10.1016/0960-1686(91)90291-E, 1991.
- Turpin, B. J., Huntzicker, J. J., and Hering, S. V.: Investigation of organic aerosol sampling artifacts in the Los Angeles basin, *Atmos. Environ.*, 28, 3061-3071, doi: 10.1016/1352-2310(94)00133-6, 1994.
- Turpin, B. J., Saxena, P., and Andrews, E.: Measuring and simulating particulate organics in the atmosphere: Problems and prospects, *Atmos. Environ.*, 34, 2983-3013, doi: 10.1016/S1352-2310(99)00501-4, 2000.
- van Donkelaar, A., Martin, R. V., Brauer, M., Kahn, R., Levy, R., Verduzco, C., and Villeneuve, P. J.: Global estimates of ambient fine particulate matter concentrations from satellite-based aerosol optical depth: Development and application, *Environ. Health. Perspect.*, 118, 847-855, doi: 10.1289/ehp.0901623, 2010.
- Venkatachari, P., Zhou, L., Hopke, P. K., Schwab, J. J., Demerjian, K. L., Weimer, S., Hogrefe, O., Felton, D., and Rattigan, O.: An intercomparison of measurement methods for carbonaceous aerosol in the ambient air in New York City, *Aerosol Sci. Technol.*, 40(10), 788-795, doi: 10.1080/02786820500380289, 2006.
- Volkamer, R., Jimenez, J. L., San Martini, F., Dzepina, K., Zhang, Q., Salcedo, D., Molina, L. T., Worsnop, D. R., and Molina, M. J.: Secondary organic aerosol formation from anthropogenic air pollution: Rapid and higher than expected, *Geophys. Res. Lett.*, 33, doi: 10.1029/2006GL026899, 2006.
- Wang, Y., Zhuang, G., Zhang, X., Huang, K., Xu, C., Tang, A., Chen, J., and An, Z.: The ion chemistry, seasonal cycle, and sources of PM<sub>2.5</sub> and TSP aerosol in Shanghai, *Atmos. Environ.*, 40, 2935-2952, doi: 10.1016/j.atmosenv.2005.12.051, 2006.

- Wood, S. N.: Fast stable restricted maximum likelihood and marginal likelihood estimation of semiparametric generalized linear models, *J. R. Stat. Soc.: Series B*, 73, 3-36, doi: 10.1111/j.1467-9868.2010.00749.x, 2011.
- Wu, C., Huang, X. H. H., Ng, W. M., Griffith, S. M., and Yu, J. Z.: Inter-comparison of NIOSH and  
5 IMPROVE protocols for OC and EC determination: Implications for inter-protocol data conversion, *Atmos. Meas. Tech.*, 9, 4547-4560, doi: 10.5194/amt-9-4547-2016, 2016.
- Yang, F., He, K., Ye, B., Chen, X., Cha, L., Cadle, S. H., Chan, T., and Mulawa, P. A.: One-year record of organic and elemental carbon in fine particles in downtown Beijing and Shanghai, *Atmos. Chem. Phys.*, 5, 1449-1457, doi: 10.5194/acp-5-1449-2005, 2005.
- 10 Yang, F., Huang, L., Duan, F., Zhang, W., He, K., Ma, Y., Brook, J. R., Tan, J., Zhao, Q., and Cheng, Y.: Carbonaceous species in PM<sub>2.5</sub> at a pair of rural/urban sites in Beijing, 2005-2008, *Atmos. Chem. Phys.*, 11, 7893-7903, doi: 10.5194/acp-11-7893-2011, 2011.
- Yu, X. Y., Cary, R. A., and Laulainen, N. S.: Primary and secondary organic carbon downwind of Mexico City, *Atmos. Chem. Phys.*, 9, 6793-6814, doi: 10.5194/acp-9-6793-2009, 2009.
- 15 Zhang, B., Cao, C., Hughes, R. M., and Davis, W. S.: China's new environmental protection regulatory regime: Effects and gaps, *J Environ Manage*, 187, doi: 10.1016/j.jenvman.2016.11.009, 2017.
- Zhang, X. Y., Wang, Y. Q., Zhang, X. C., Guo, W., and Gong, S. L.: Carbonaceous aerosol composition over various regions of China during 2006, *J. Geophys. Res.*, 113, doi: 10.1029/2007JD009525, 2008a.
- 20 Zhang, X. Y., Wang, Y. Q., Zhang, X. C., Guo, W., and Gong, S. L.: Carbonaceous aerosol composition over various regions of China during 2006, *J. Geophys. Res.*, 113, doi: 10.1029/2007JD009525, 2008b.
- Zhang, Y. L., and Cao, F.: Is it time to tackle PM<sub>2.5</sub> air pollutions in China from biomass-burning emissions?, *Environ. Pollut.*, 202, 217-219, doi: 10.1016/j.envpol.2015.02.005, 2015.
- 25 Zhang, Y. L., Perron, N., Ciobanu, V. G., Zotter, P., Minguillon, M. C., Wacker, L., Prevot, A. S. H., Baltensperger, U., and Szidat, S.: On the isolation of OC and EC and the optimal strategy of radiocarbon-based source apportionment of carbonaceous aerosols, *Atmos. Chem. Phys.*, 12, 10841-10856, doi: 10.5194/acp-12-10841-2012, 2012.
- Zhang, Y. L., Huang, R. J., El Haddad, I., Ho, K. F., Cao, J. J., Han, Y., Zotter, P., Bozzetti, C.,  
30 Daellenbach, K. R., Canonaco, F., Slowik, J. G., Salazar, G., Schwikowski, M., Schnelle-Kreis, J., Abbaszade, G., Zimmermann, R., Baltensperger, U., Prévôt, A. S. H., and Szidat, S.: Fossil vs. non-fossil sources of fine carbonaceous aerosols in four Chinese cities during the extreme winter haze episode of 2013, *Atmos. Chem. Phys.*, 15, 1299-1312, doi: 10.5194/acp-15-1299-2015, 2015a.
- 35 Zhang, Y. L., Li, J., Zhang, G., Zotter, P., Huang, R. J., Tang, J. H., Wacker, L., Prevot, A. S. H., and Szidat, S.: Radiocarbon-based source apportionment of carbonaceous aerosols at a regional background site on Hainan Island, South China, *Environ. Sci. Technol.*, 48, 2651-2659, doi: 10.1021/es4050852, 2014.
- Zhang, Y. L., Schnelle-Kreis, J., Abbaszade, G., Zimmermann, R., Zotter, P., Shen, R. R., Schafer, K.,  
Shao, L. Y., Prevot, A. S. H., and Szidat, S.: Source apportionment of elemental carbon in Beijing,  
40 China: Insights from radiocarbon and organic marker measurements, *Environ. Sci. Technol.*, 49, 8408-8415, doi: 10.1021/acs.est.5b01944, 2015b.
- Zhang, Y. L., Kawamura, K., Agrios, K., Lee, M., Salazar, G., and Szidat, S.: Fossil and nonfossil sources of organic and elemental carbon aerosols in the outflow from Northeast China, *Environ. Sci. Technol.*, 50, 6284-6292, doi: 10.1021/acs.est.6b00351, 2016.

- Zhao, H. Y., Zhang, Q., Guan, D. B., Davis, S. J., Liu, Z., Huo, H., Lin, J. T., Liu, W. D., and He, K. B.: Assessment of China's virtual air pollution transport embodied in trade by using a consumption-based emission inventory, *Atmos. Chem. Phys.*, 15, 5443-5456, 10.5194/acp-15-5443-2015, 2015.
- 5 Zhao, Y., Zhang, J., and Nielsen, C. P.: The effects of recent control policies on trends in emissions of anthropogenic atmospheric pollutants and CO<sub>2</sub> in China, *Atmos. Chem. Phys.*, 13, 487-508, doi: 10.5194/acp-13-487-2013, 2013.
- Zheng, M., Salmon, L. G., Schauer, J. J., Zeng, L., Kiang, C. S., Zhang, Y., and Cass, G. R.: Seasonal trends in PM<sub>2.5</sub> source contributions in Beijing, China, *Atmos. Environ.*, 39, 3967-3976, doi: 10.1016/j.atmosenv.2005.03.036, 2005.
- 10 Zielinska, B., Sagebiel, J., McDonald, J. D., Whitney, K., and Lawson, D. R.: Emission rates and comparative chemical composition from selected in-use diesel and gasoline-fueled vehicles, *J. Air Waste Manage. Assoc.*, 54, 1138-1150, doi: 10.1080/10473289.2004.10470973, 2004.

15

20

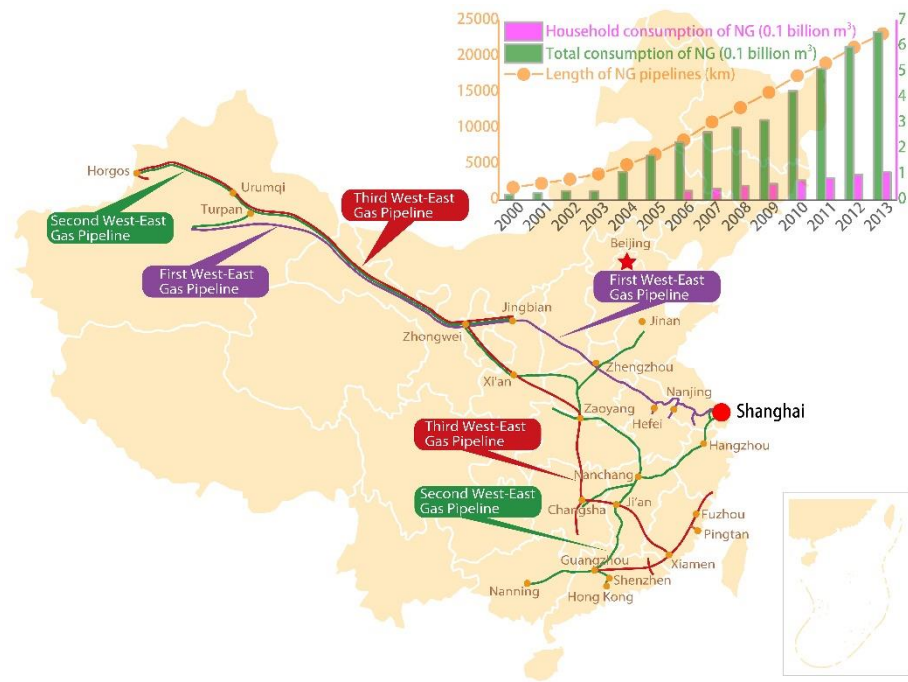


**Figure 1.** Every pipeline leads to Shanghai. The west-east pipeline project (WEPP) is a set of natural gas pipelines which transport clean natural gas from Xinjiang to the energy-hungry Yangtze River Delta region (including Shanghai). Started in 2002, the construction of the WEPP is one of China's largest energy infrastructures. The first, second, and third pipelines were completed in 2005, 2011, and 2015, respectively. The figure at the top right shows the rapid increase of pipeline construction and natural gas consumption in Shanghai between 2000 and 2013 (Wen, 2014).

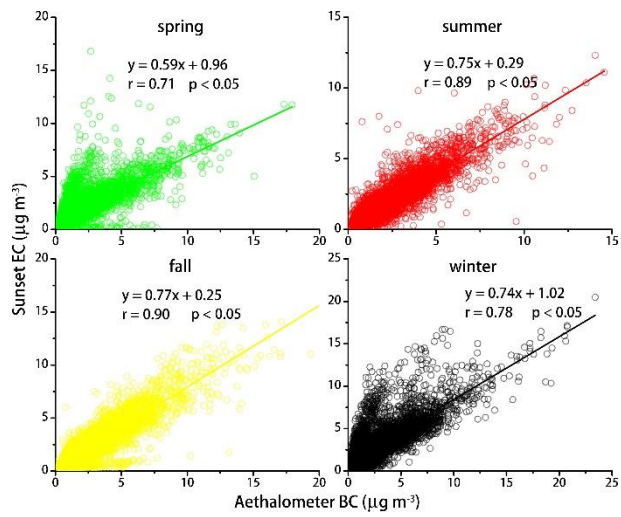


**Figure 2.** Comparison between collocated Aethalometer BC and Sunset EC concentrations for different seasons.

5

10

15

20



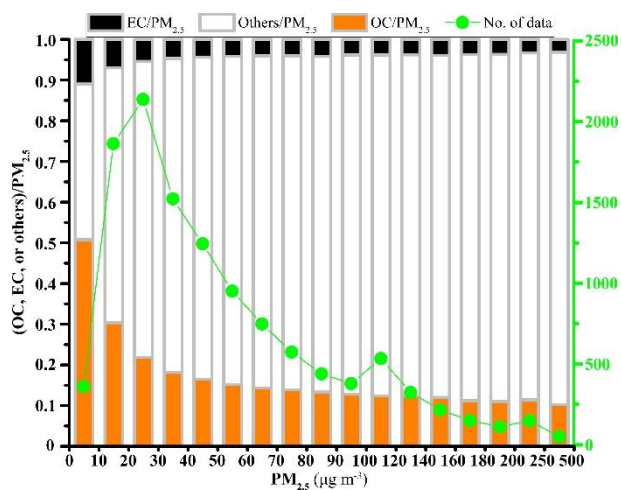


**Figure 3.** The contribution fraction of OC, EC, and other aerosol species to ambient PM<sub>2.5</sub> at different PM<sub>2.5</sub> concentration intervals in Shanghai between January 2013 to December 2014.

5

10

15

20

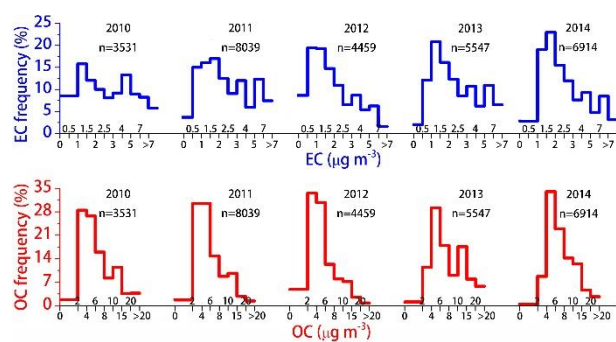


**Figure 4.** Frequency of EC and OC mass loadings in five different years in Shanghai. The frequency was calculated based on the average data points within a mass concentration interval of  $0.5 \mu\text{g m}^{-3}$  and  $2 \mu\text{g m}^{-3}$  for EC and OC, respectively.

5

10

15

20

25

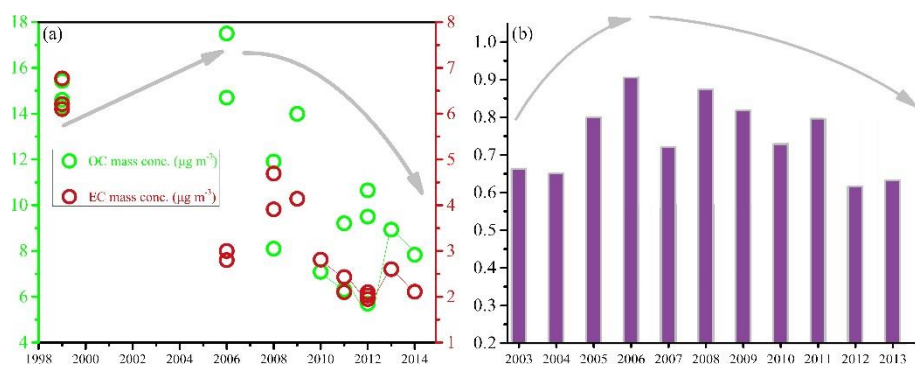


**Figure 5.** Long-term evolution of annual carbonaceous aerosol concentrations **(a)** and MODIS-derived aerosol optical depth **(b)** in Shanghai. Note that the line-collected circles in the left figure represent the results in this study, the sources of the rest circles are listed in SI Table S1.

5

10

15

20

25

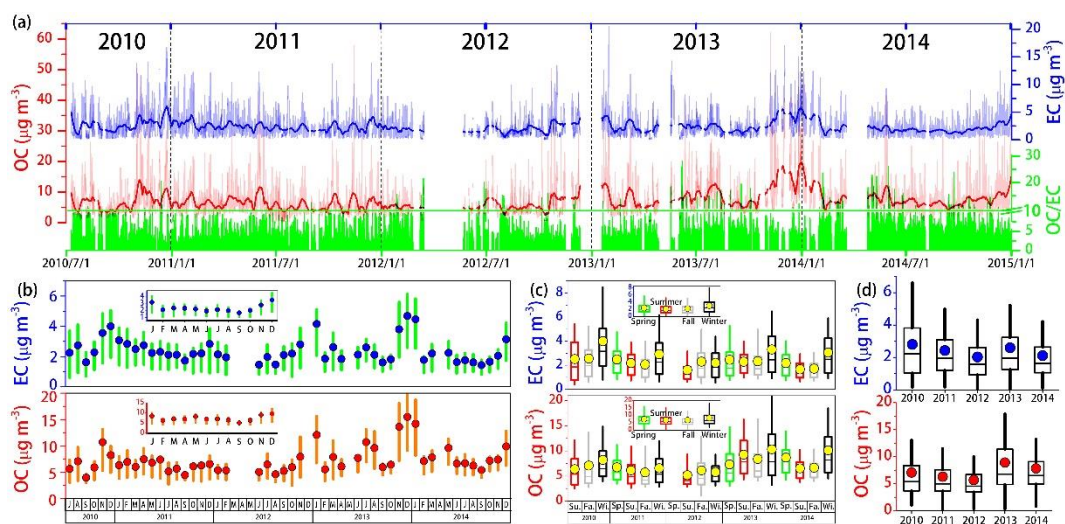


**Figure 6.** Hourly (a), monthly (b), seasonal (c), and interannual (d) variations of OC and EC mass concentrations in Shanghai. Note that the variations of OC/EC are also shown in a, setting 10 as the breaking point. The relatively small figures in b and c represent the overall monthly and seasonal mass concentrations of OC and EC throughout our study period, respectively.

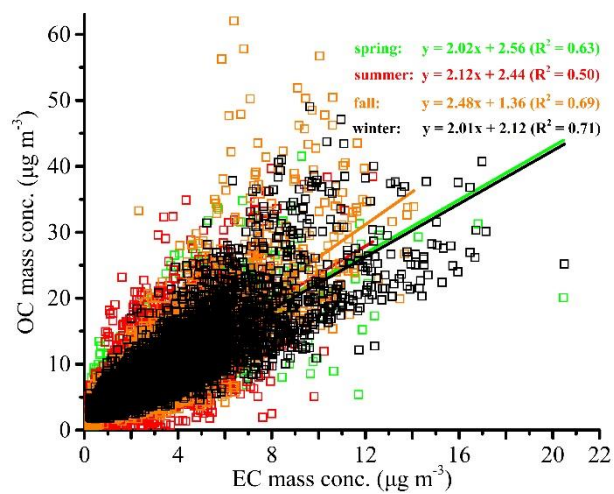


**Figure 7.** Correlation between EC and OC mass concentrations during different seasons in Shanghai.

5

10

15

20

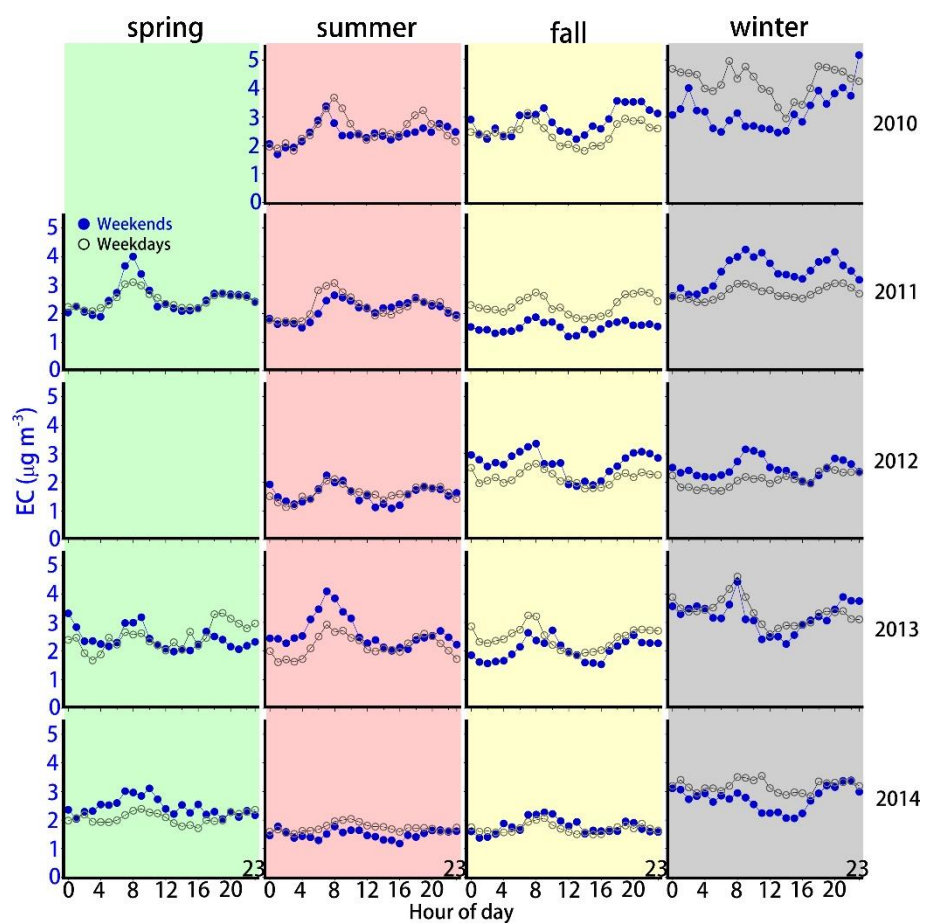


**Figure 8.** Diurnal variations of EC concentrations during weekdays and weekends over different years in Shanghai.

5

10

15

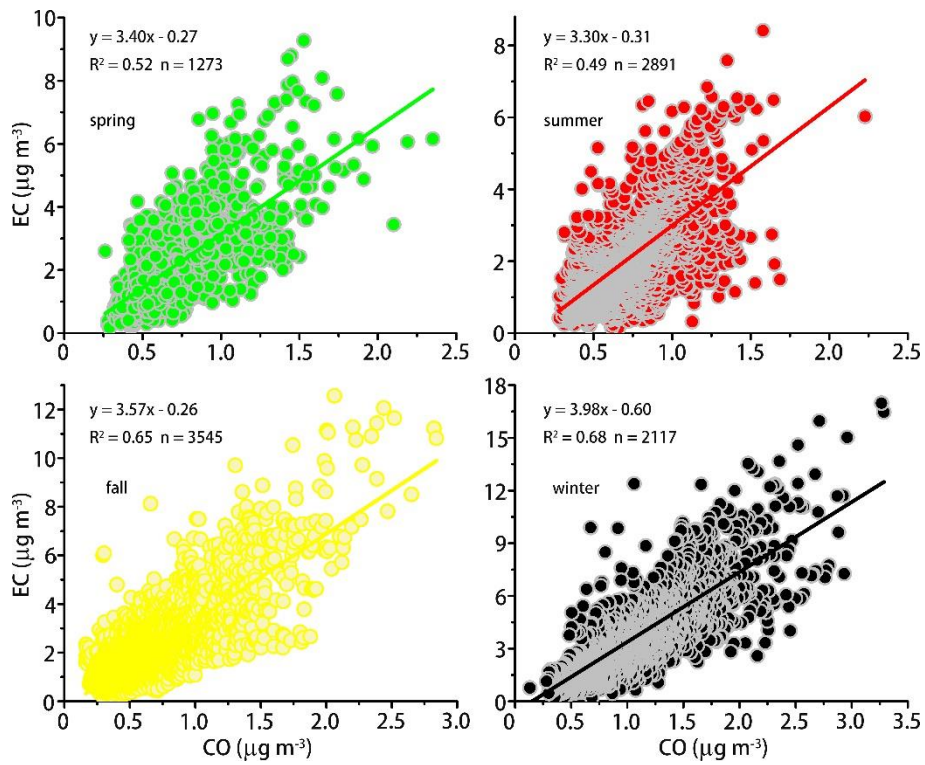


**Figure 9.** Correlation analysis of the mass concentrations of CO and EC during four seasons in Shanghai.

5

10

15

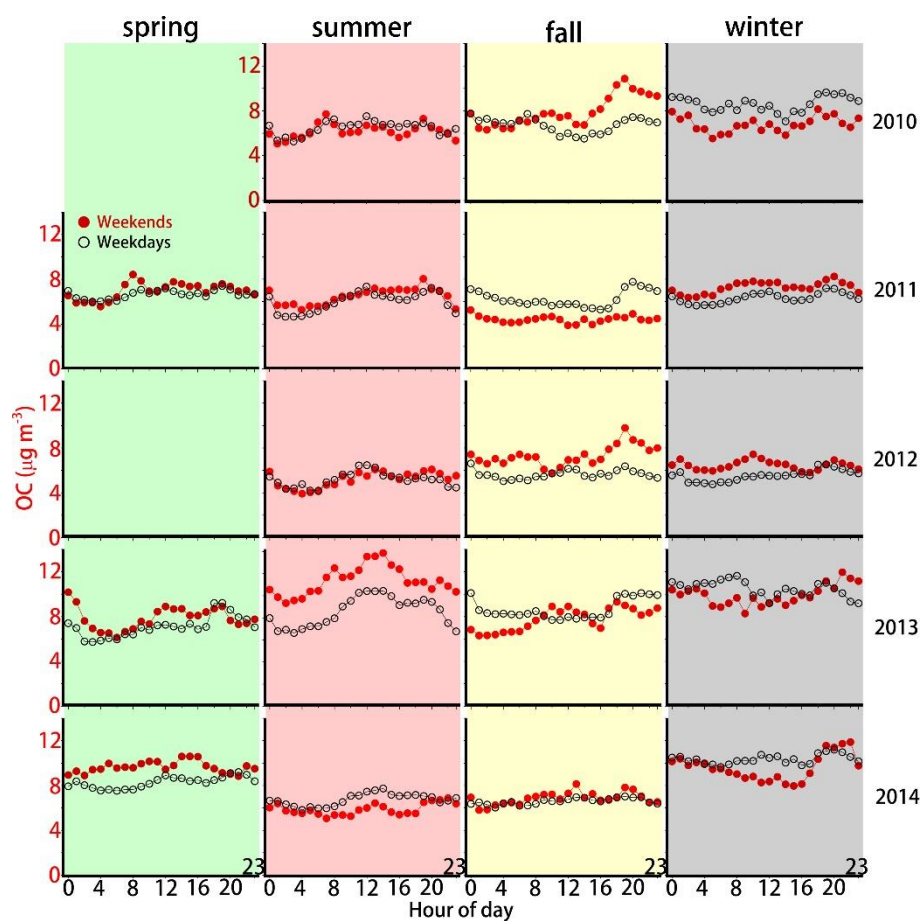


**Figure 10.** Diurnal variations of OC concentrations during weekdays and weekends over different years in Shanghai.

5

10

15



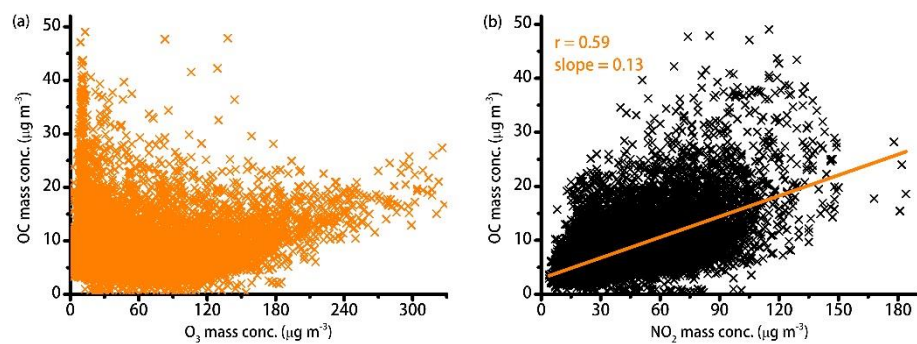


**Figure 11.** Scatter plots of OC vs. O<sub>3</sub> (a) and OC vs. NO<sub>2</sub> (b) in Shanghai.

5

10

15

20

25

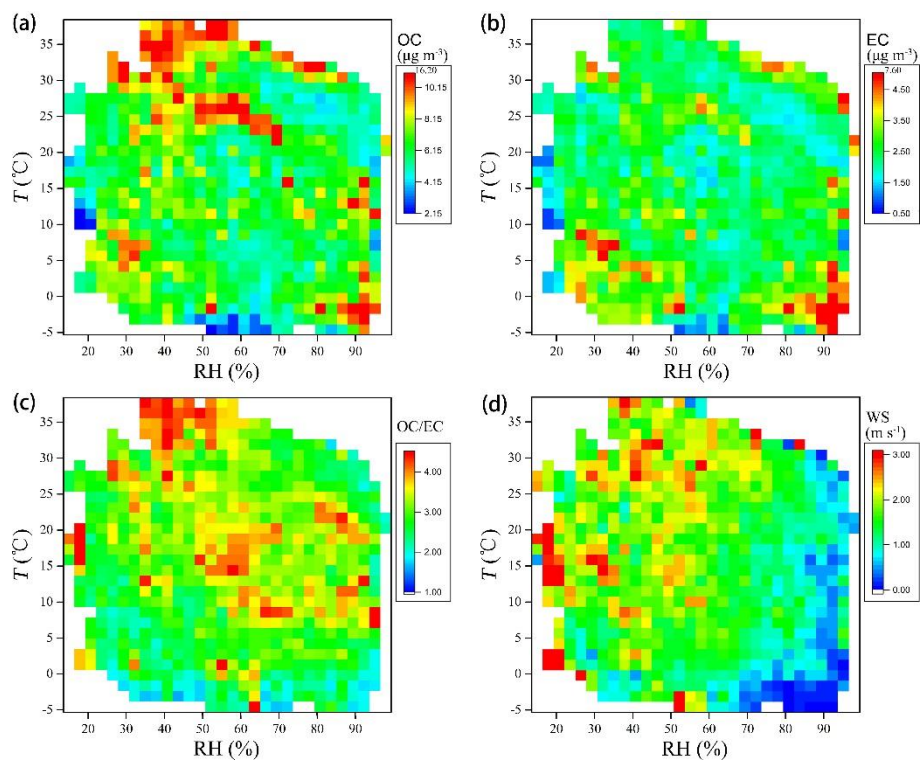


**Figure 12.** RH/ $T$  dependence of (a) OC mass concentrations, (b) EC mass concentrations, (c) OC/EC ratios, and (d) wind speeds (WS) between July 2010 and December 2014 in Shanghai. The data are grouped into 900 (30\*30) grids with increments of RH and  $T$  being 2.86% and 1.46 °C, respectively.

5

10

15

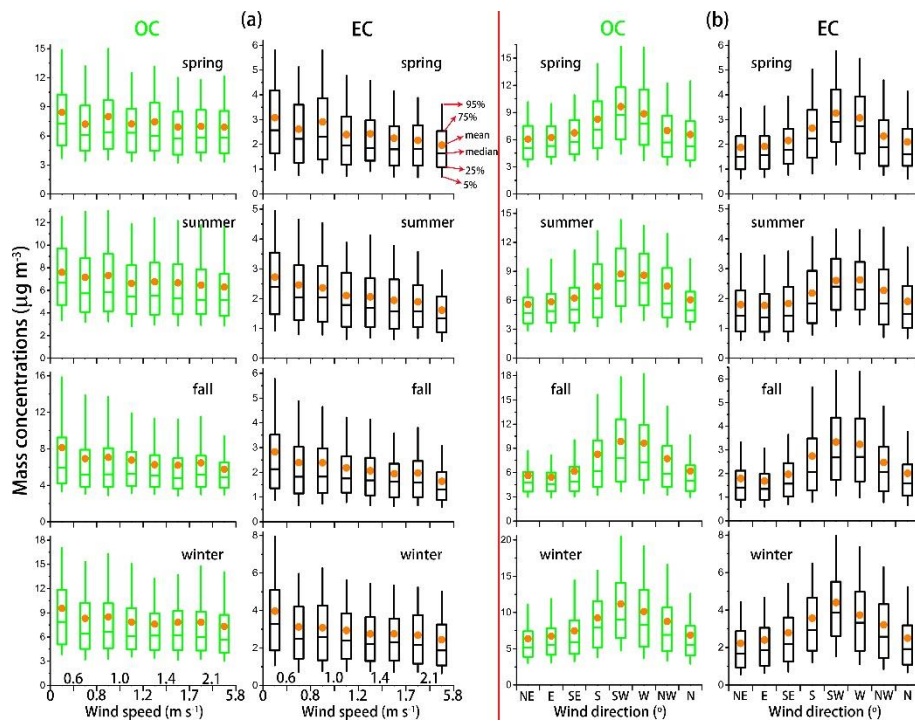


**Figure 13.** Box plots of OC and EC mass concentrations as a function of wind speed increments **(a)** and wind direction sectors **(b)** between July 2010 and December 2014 in Shanghai. The mean, median, 5<sup>th</sup>, 25<sup>th</sup>, 75<sup>th</sup> and 95<sup>th</sup> percentiles are indicated in the second figure of the top row.

5

10

15

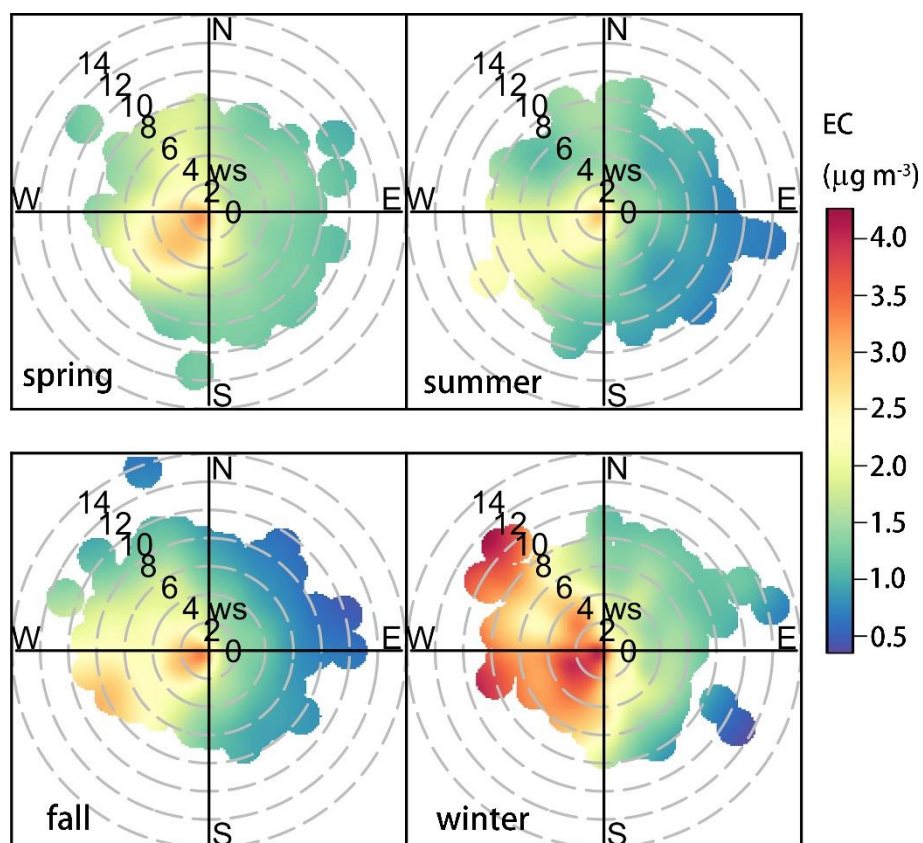


**Figure 14.** Bivariate polar plots of seasonal EC concentrations ( $\mu\text{g m}^{-3}$ ) in Shanghai between July 2010 and December 2014. The center of each plot represents a wind speed of zero, which increases radially outward. The concentration of EC is shown by the colour scale.

5

10

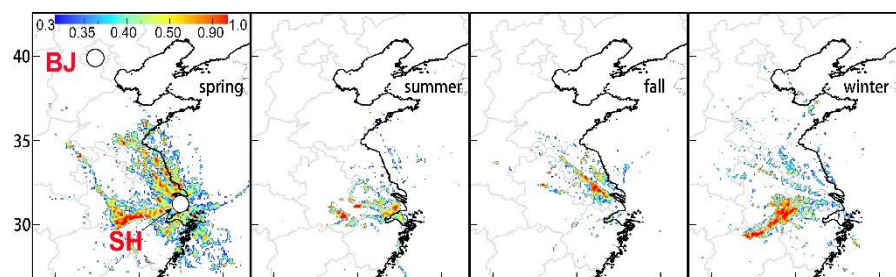


**Figure 15.** Potential Source Contribution Function (PSCF) of OC during four seasons in 2014 in Shanghai. The cities marked in the leftmost panel are Beijing (BJ) and Shanghai (SH). The colour scales indicate the values of PSCF.

5

10

15

20

25

**Table 1.** Descriptive statistics of the annual and seasonal variations of EC, OC, and OC/EC during 10 July 2010-31 December 2014 in Shanghai. Note that the statistics result of 2012 spring is not given due to data deficiency.

	Year	Season	N	Mean	SD	Min	P5	Q1	Median	Q3	P95	Max
EC	2010	annual	3531	2.81	2.39	0.17	0.39	1.03	2.23	3.82	7.41	16.72
		Summer	1050	2.52	2.02	0.17	0.32	0.76	1.87	3.92	6.32	10.68
		Fall	1846	2.56	2.12	0.24	0.45	1.06	1.96	3.28	6.89	14.07
		Winter	635	4.00	3.18	0.22	0.57	1.93	3.17	5.06	11.48	16.72
	2011	annual	8039	2.43	1.80	0.19	0.55	1.21	1.94	3.10	6.12	13.94
		Spring	2128	2.49	1.61	0.23	0.64	1.35	2.12	3.16	5.80	12.11
		Summer	1903	2.19	1.40	0.22	0.60	1.18	1.86	2.91	4.74	12.32
		Fall	1940	2.07	1.62	0.19	0.50	1.02	1.69	2.47	5.37	13.68
		Winter	2068	2.92	2.29	0.22	0.50	1.25	2.28	3.86	7.84	13.94
	2012	annual	4459	2.03	1.59	0.07	0.37	0.93	1.57	2.62	5.31	13.47
		Spring	192									
		Summer	1259	1.61	1.19	0.16	0.53	0.87	1.23	1.88	4.05	9.86
		Fall	1520	2.30	1.89	0.07	0.28	1.02	1.75	3.02	6.11	13.47
		Winter	1488	2.20	1.52	0.22	0.45	1.00	1.86	3.00	5.31	8.70
	2013	annual	5547	2.60	2.07	0.06	0.70	1.26	1.97	3.24	6.60	20.49
		Spring	1080	2.46	2.13	0.06	0.48	1.13	1.74	3.08	6.56	20.46
		Summer	1570	2.29	1.31	0.16	0.77	1.34	2.03	2.89	4.85	8.41
		Fall	1465	2.33	1.84	0.29	0.76	1.20	1.72	2.71	6.46	12.56
		Winter	1432	3.32	2.68	0.20	0.72	1.41	2.46	4.39	8.63	20.49
	2014	annual	6914	2.11	1.55	0.12	0.60	1.06	1.64	2.64	5.24	12.41
		Spring	1284	2.19	1.43	0.18	0.57	1.14	1.83	2.86	5.10	9.27
		Summer	1829	1.67	0.98	0.15	0.52	0.96	1.43	2.17	3.58	6.17
		Fall	2144	1.72	1.09	0.12	0.58	0.99	1.43	2.14	3.98	9.01
		Winter	1657	3.06	2.14	0.21	0.77	1.35	2.50	4.25	7.12	12.41

OC	2010	annual	3531	7.09	5.50	1.06	2.41	3.69	5.39	8.38	17.74	50.46
		Summer	1050	6.39	4.00	1.06	2.07	3.31	5.36	8.40	14.02	26.32
		Fall	1846	7.09	6.28	1.66	2.47	3.56	4.92	7.69	20.11	50.46
		Winter	635	8.22	5.04	1.99	3.36	4.91	6.48	9.98	20.26	30.30
		annual	8039	6.31	4.25	0.20	2.55	3.68	5.00	7.59	14.21	57.81
	2011	Spring	2128	6.74	3.68	2.11	3.15	4.23	5.71	8.06	13.80	33.92
		Summer	1903	6.14	4.58	0.20	1.91	3.51	4.84	7.29	13.77	38.45
		Fall	1940	5.73	4.83	1.18	2.56	3.39	4.21	5.83	14.86	57.81
		Winter	2068	6.58	3.81	1.69	2.49	3.79	5.36	8.40	14.39	25.12
		annual	4459	5.70	3.79	0.38	2.12	3.48	4.56	6.75	13.26	50.32
	2012	Spring	192									
		Summer	1259	5.19	3.00	1.74	2.64	3.39	4.11	5.66	11.54	21.87
		Fall	1520	6.14	4.97	0.38	0.74	3.33	4.58	7.60	15.71	50.32
		Winter	1488	5.81	2.94	1.76	2.68	3.90	4.99	6.99	11.29	30.17
		annual	5547	8.93	6.18	0.36	3.08	4.88	6.79	11.39	20.88	62.05
	2013	Spring	1080	7.31	4.97	0.36	2.40	4.02	5.61	9.41	18.47	31.32
		Summer	1570	9.27	5.04	1.11	3.87	5.51	7.82	12.05	18.75	39.66
		Fall	1465	8.40	6.32	2.49	3.76	4.89	6.02	9.28	20.57	62.05
		Winter	1432	10.33	7.50	2.03	2.82	5.14	7.86	13.29	26.28	49.03
		annual	6914	7.83	4.55	0.81	3.66	4.95	6.52	9.09	17.01	47.10
	2014	Spring	1284	8.69	4.52	1.16	3.78	5.62	7.86	10.16	17.50	41.53
		Summer	1829	6.53	2.85	0.81	3.37	4.55	5.83	7.79	11.93	25.14
		Fall	2144	6.67	3.23	0.85	3.70	4.72	5.77	7.49	12.89	34.98
		Winter	1657	10.13	6.22	2.27	3.98	5.67	8.19	12.82	22.39	47.10
		annual	3531	3.41	2.07	0.62	1.34	2.01	2.73	4.08	8.27	20.46
OC/EC	2010	Summer	1050	3.80	2.37	0.62	1.16	2.08	3.03	4.94	9.07	10.82
		Fall	1846	3.40	1.90	0.66	1.38	2.18	2.86	3.95	7.86	11.39
		Winter	635	2.80	1.88	0.98	1.47	1.77	2.08	2.81	6.96	20.46
		annual	8039	3.16	1.63	0.11	1.50	2.10	2.67	3.62	6.76	12.43
	2011	annual	8039	3.16	1.63	0.11	1.50	2.10	2.67	3.62	6.76	12.43

	Spring	2128	3.19	1.43	0.89	1.71	2.30	2.82	3.54	6.35	10.08
	Summer	1903	3.19	1.66	0.11	1.04	2.11	2.88	3.88	6.59	12.43
	Fall	1940	3.29	1.72	1.06	1.60	2.11	2.70	3.85	7.05	10.99
	Winter	2068	2.98	1.71	0.92	1.51	1.91	2.40	3.17	7.02	9.98
	annual	4459	3.53	2.04	0.34	1.73	2.23	2.89	4.06	7.95	21.67
2012	Spring	192									
	Summer	1259	3.88	1.99	0.34	1.84	2.75	3.47	4.42	7.39	20.34
	Fall	1520	2.97	1.26	0.82	1.65	2.21	2.69	3.42	5.13	15.88
	Winter	1488	3.62	2.36	0.98	1.75	2.08	2.50	4.42	8.85	15.46
	annual	5547	3.92	1.76	0.46	2.05	2.83	3.57	4.59	6.71	28.04
2013	Spring	1080	3.51	1.52	0.46	1.79	2.58	3.23	4.05	6.30	18.50
	Summer	1570	4.49	2.20	1.13	2.28	3.23	4.08	5.17	7.73	28.04
	Fall	1465	4.02	1.58	1.11	2.32	2.99	3.72	4.64	6.67	19.51
	Winter	1432	3.49	1.30	1.13	2.00	2.60	3.25	4.11	5.81	13.84
	annual	6914	4.40	1.90	0.70	2.33	3.17	4.00	5.16	7.83	26.14
2014	Spring	1284	4.76	2.30	1.05	2.46	3.27	4.24	5.69	8.50	26.14
	Summer	1829	4.55	1.90	0.96	2.31	3.35	4.16	5.28	8.25	18.54
	Fall	2144	4.51	1.79	0.70	2.40	3.33	4.23	5.33	7.59	24.01
	Winter	1657	3.83	1.52	1.03	2.25	2.89	3.52	4.35	6.41	23.72
	annual										